Title

COMPETITION BETWEEN ATOMIC AND MOLECULAR CHLORINE ELIMINATION IN THE INFRARED MULTIPHOTON DISSOCIATION OF CF2Cl2

Author

Krajnovich, D.

Publication Date

1982-05-01

LBL-14478
Preprint

Lawrence Berkeley Laboratory
UNIVERSITY OF CALIFORNIA

Materials & Molecular
Research Division

Submitted to the Journal of Chemical Physics

COMPETITION BETWEEN ATOMIC AND MOLECULAR CHLORINE ELIMINATION IN THE INFRARED MULTIPHOTON DISSOCIATION OF CF_2Cl_2

D. Krajnovich, F. Huisken, Z. Zhang,
Y.R. Shen, and Y.T. Lee

May 1982

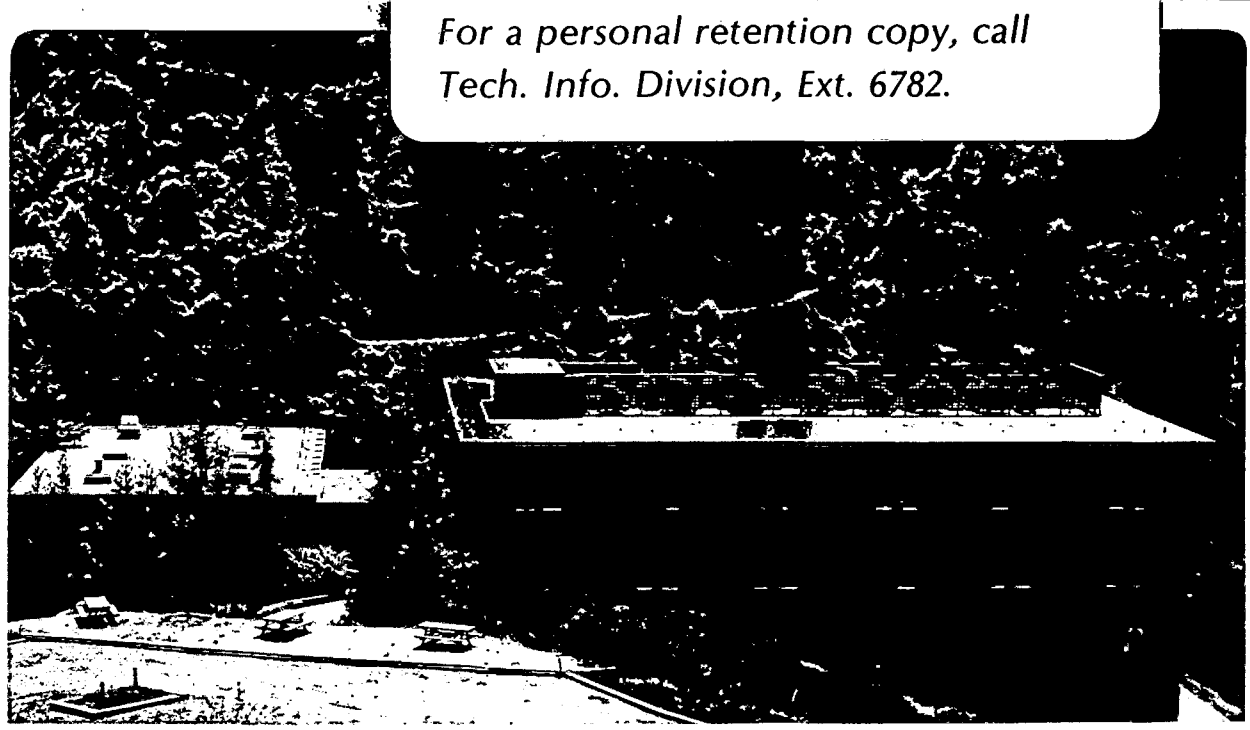

Prepared for the U.S. Department of Energy under Contract DE-AC03-76SF00098

DISCLAIMER

COMPETITION BETWEEN ATOMIC AND MOLECULAR CHLORINE ELIMINATION IN THE INFRARED MULTIPHOTON DISSOCIATION OF CF_2Cl_2

D. Krajnovich[a], F. Huisken[b], Z. Zhang[c], Y. R. Shen[d] and Y. T. Lee[a,e]

Materials and Molecular Research Division
Lawrence Berkeley Laboratory
University of California
Berkeley, CA 94720

ABSTRACT

Infrared multiphoton dissociation of CF_2Cl_2 has been reinvestigated by the crossed laser-molecular beam technique using a high repetition rate CO_2 TEA laser. Both the atomic and molecular chlorine elimination channels were observed: (1) $CF_2Cl_2 \rightarrow CF_2Cl + Cl$, and (2) $CF_2Cl_2 \rightarrow CF_2 + Cl_2$. No evidence was found for secondary dissociation of CF_2Cl at laser energy fluences up to 8 J/cm^2. Center-of-mass product translational energy distributions were obtained for both dissociation channels. In agreement with previous work, the products of reaction (1) are found to have a statistical translational energy distribution. The products of reaction (2) are formed with a mean translational energy of 8 kcal/mole, and the distribution peaks rather sharply about this value, indicating a sizeable exit barrier to molecular elimination. The product branching ratio was directly determined. Reaction (2) accounts for roughly 10% of the total dissociation yield in the fluence range 0.5 - 8 J/cm^2. These results provide an additional test of the statistical theory of unimolecular reactions.

This work was supported by the Director, Office of Energy Research, Office of Basic Energy Sciences, Chemical Sciences Division and the Assistant Secretary for Nuclear Energy, Office of Advanced Systems and Nuclear Projects, Advanced Isotope Separation Division of the U.S. Department of Energy under Contract DE-AC03-76SF00098.

I. INTRODUCTION

Infrared multiphoton absorption may be used to prepare vibrationally excited molecules for studies of unimolecular reaction dynamics. CF_2Cl_2 is a particularly interesting candidate for such studies, since it has two dissociation channels with nearly the same endothermicity:

(1) $CF_2Cl_2 \longrightarrow CF_2Cl + Cl$ $\quad \Delta H = 80$ kcal/mole

(2) $\longrightarrow CF_2 + Cl_2$ $\quad \Delta H = 73$ kcal/mole

The threshold energy for reaction (2) is expected to be somewhat higher than the endothermicity, since there probably exists an activation energy for the reverse association reaction.

In order to gain a basic understanding of the dissociation dynamics of this simple system, the following questions must be answered. (1) What is the size of the potential energy barrier in the molecular elimination channel? (Does that channel have a lower or higher threshold energy than the atomic elimination channel?) (2) How many photons do the molecules absorb before they dissociate, and what do the product energy distributions look like? (3) What is the branching ratio and how does it depend on the laser intensity and energy fluence? Are the results in quantitative agreement with the predictions of RRKM theory? (4) Is secondary dissociation of CF_2Cl important?

Recently a number of experiments on CF_2Cl_2 have been reported which bear on these questions. In a previous molecular beam experiment,[1] only the atomic elimination reaction was observed and the translational energy distribution of the $CF_2Cl + Cl$ products was measured. It was inferred that the molecules absorb, on average, 2-3

photons beyond the threshold for reaction (1). An upper limit of 10% was placed on the fraction of molecules dissociating via Cl_2 elimination.

King and Stephenson[2] used the laser-induced fluorescence (LIF) technique to measure the initial internal energy distribution of the CF_2 fragments produced in reaction (2). An optical time-of-flight (TOF) method was also used[3] to estimate the average kinetic energy of the nascent CF_2 products. Since only CF_2 was detected in these experiments, no estimate of the relative importance of reactions (1) and (2) could be made. Also, the possibility that some of the CF_2 was created by secondary dissociation of CF_2Cl, although unlikely, could not be completely ruled out. Of course, such interference would greatly complicate and dilute the significance of their results.

Hudgens[4] used a beam sampling mass spectrometer to measure the real-time mass spectra of CF_2Cl_2 photolysis products following a CO_2 laser pulse. He observed signals from masses 70, 72 and 74, corresponding to Cl_2 formation with a normal isotopic distribution. By comparing the relative signals at masses 70 and 35 (after suitable corrections), he estimated the ratio of Cl versus Cl_2 formation to be greater than 33:1. However, this estimate may not be valid if there is a significant difference in the amount of translational energy released in reactions (1) and (2), since the kinematics of the dissociation process affects the detection sensitivity.

A large number of conventional gas cell photolysis experiments have also been performed on CF_2Cl_2. In one study, Morrison and Grant[5]

used Br_2 as a scavenger in ten-fold excess over CF_2Cl_2. Following irradiation, only two products were observed, CF_2ClBr and CF_2Br_2, which they interpreted as arising from CF_2Cl and CF_2, respectively. They found that the CF_2 yield comprised only 4% of the total dissociation yield at a laser energy fluence of 6 J/cm^2 and that this percentage increased as the fluence was lowered. This suggests that reaction (2), rather than secondary dissociation of CF_2Cl, is the dominant source of CF_2 in this fluence range. As the fluence was lowered further, the relative CF_2 yield passed through a maximum (~7% of the total) and then decreased. From this Morrison and Grant concluded that the threshold for Cl_2 elimination (endoergicity + barrier) must be higher than that for C-Cl bond fission. Such a conclusion must be regarded cautiously, since collisional effects are certainly important, even during the laser pulse, at the relatively high pressures (1 torr) of these experiments.

In the present molecular beam experiment, a high repetition rate CO_2 TEA laser was used as the excitation source. The two orders-of-magnitude increase in duty cycle over the previous molecular beam experiment allowed both dissociation channels to be observed. The experiment consisted mainly of (1) measurement of the product translational energy distributions for both dissociation channels, (2) accurate determination of the branching ratio and its dependence on energy fluence, and (3) estimation of the importance of secondary dissociation of CF_2Cl. The results clear up some of the ambiguities in the previous experiments, and allow us to give quantitative answers to most of the questions posed earlier.

II. EXPERIMENTAL ARRANGEMENT

The molecular beam apparatus used in this study has been described in detail previously.[6] Briefly, a supersonic beam of CF_2Cl_2 molecules was crossed at right angles with the output of a high repetition rate CO_2 TEA laser in a liquid nitrogen cooled interaction chamber maintained at ~5 x 10^{-7} torr. The multiphoton dissociation products were detected in the plane of the laser and molecular beams by a rotatable, ultra-high vacuum mass spectrometer consisting of a triply differentially pumped electron bombardment ionizer, a quadrupole mass filter, and a Daly-type ion counter.

The molecular beam was formed by expanding 200 torr of neat CF_2Cl_2 through a 0.1 mm diameter quartz nozzle, which was heated to 180°C to enhance multiphoton absorption. The velocity distribution of this CF_2Cl_2 beam was determined by conventional TOF measurements. The beam had a peak velocity of 5.45 x 10^4 cm/sec and a FWHM velocity spread of 30%. The molecular beam source utilized three stages of differential pumping to reduce the amount of effusive background entering the detector at small viewing angles. The beam was defined to an angular divergence of ~1.5°.

A GenTec DD-250 CO_2 TEA laser was used as the excitation source. The laser was tuned to 1083 cm^{-1} for all of the measurements reported here. This excites the ν_1 mode of CF_2Cl_2 which is centered at 1098 cm^{-1}.[7] The energy fluence was adjusted by varying the distance between a 25 cm focal length ZnSe lens and the molecular beam. The

multimode laser pulses had a FWHM of ~150 ns with very little tail. Typically the laser produced 0.3 J/pulse at a repetition rate of 70 Hz.

Angular distributions of the multiphoton dissociation products were measured as a function of the angle θ between the detector and the molecular beam. The effective angular resolution of the detector is between 1.2° and 3.5°, depending on the size of the interaction region. At a given angle θ, the signal $N(\theta)$ was measured by gating two scalers with a reference pulse from the CO_2 laser. After an initial delay (to allow the fastest fragments to almost reach the detector), the first scaler was enabled to count signal plus background for a gate width corresponding to the width of the TOF distribution. After a long (10 ms) delay, the second scaler was enabled to count for an equal period of time. This allowed background subtraction.

Product TOF distributions at various angles were obtained using a 255-channel multiscaler interfaced to a Digital Equipment Corporation LSI-11 microcomputer. The reference pulse from the laser served to trigger the scaler. A dwell time per channel of 10 μs was used.

III. RESULTS AND ANALYSIS

In order to unambiguously study a system with two competing dissociation channels, we need to be able to detect, without interference, at least one product from each dissociation channel. This is possible in the present case, since the CF_2Cl and Cl_2 products of reactions (1) and (2) can be uniquely monitored as CF_2Cl^+ and Cl_2^+ in the mass spectrometer. TOF distributions of CF_2Cl^+ and Cl_2^+ obtained at $\theta = 5^\circ$ are shown in Fig. 1, proving that both reactions (1) and (2) are occurring to a measurable extent. In Parts A and B of this section we present our detailed results on the dynamics of these competing reaction channels. In Part C we estimate the importance of secondary dissociation of CF_2Cl. Finally, in part D we consider the branching ratio and its dependence on laser energy fluence. With the obvious exception of the branching ratio vs. fluence measurements, all results reported were obtained at an energy fluence of 6 J/cm^2.

A. $CF_2Cl_2 \rightarrow CF_2Cl + Cl$

The angular distribution of CF_2Cl^+ is shown in Fig. 2. The error bars represent plus and minus two standard deviations of the statistical counting error. Angular distributions of $CFCl^+$ and CF_2^+ were also measured and were found to be identical to CF_2Cl^+ within experimental error. The velocity distributions of CF_2Cl^+ at three laboratory angles are shown in Fig. 3. For clarity, all three velocity distributions have been normalized to the same height. These are velocity flux

distributions, I(v), which are related to the measured TOF (number density) distributions by

$$I(v) \propto \frac{N(t)}{v} \quad .$$

These angular and velocity distributions were used to deduce the probability distribution of the center-of-mass (CM) translational energy, P(E), released to the fragments in the dissociation process. In the analysis, an assumed P(E) is used to calculate the laboratory angular and velocity distributions of the detected fragment. These are compared to the experimental distributions. The P(E) is then modified and the calculation repeated until a good fit is obtained. Typically only two parameters are needed to fit the data; these are the peak and the width of the translational energy distribution. Center-of-mass angular distributions of the products are found to be isotropic.

The curves in Figs. 2 and 3 were calculated from the P(E)'s shown in Fig. 4. These distributions all peak at zero and have mean translational energies of 0.8, 1.4 and 2.0 kcal/mole. The theoretical and experimental angular distributions were normalized at $\theta = 20^{\circ}$. The theoretical velocity distributions were all normalized to the maximum of the experimental distribution at <u>each</u> angle (i.e., no relative normalization factors related to the theoretical angular distributions were used).

The P(E) represented by the solid curve in Fig. 4 gives the best fit to the data. The other two P(E)'s serve to illustrate the sensitivity of the fitting procedure. We conclude that the $CF_2Cl + Cl$ products are formed with a mean (CM) translational energy of ~1.4 ± 0.2 kcal/mole and

that the distribution of recoil energies peaks at or very near zero (within ~0.1 kcal/mole).

While it is well known that the primary purpose of RRKM theory is to calculate rate constants, the theory also predicts product translational energy distributions in cases where there is negligible interaction between the products after the critical configuration is passed. It has been shown[1] that this condition is often satisfied by molecules undergoing simple bond fission reactions, including CF_2Cl_2. By comparing RRKM P(E)'s with experiment, it is therefore possible to estimate the average level of molecular excitation and the dissociation lifetime.

The P(E)'s in Fig. 4 were actually calculated from RRKM theory for various levels of excitation. The present RRKM calculation is essentially identical to that described by Sudbo et al.[1] For completeness, a description of the calculation is included in Appendix I. The best fit RRKM P(E) obtains for a level of excitation of 8.0 kcal/mole (2.5 photons) above the C-Cl dissociation threshold. The corresponding dissociation lifetime is around 4 ns. Since the mean translational energy is 1.4 kcal/mole, about 6.6 kcal/mole is left in the internal degrees of freedom of the CF_2Cl product.

Angular and velocity distributions of Cl^+ were also measured. These are shown in Figs. 5 and 6. The angular distribution of Cl^+ is significantly narrower than the angular distribution of Cl calculated from the P(E) which best fit the CF_2Cl^+ data. This indicates that an appreciable fraction of the CF_2Cl radicals which are ionized crack to

give Cl^+. (Cl_2 produced in reaction (2) is also a source of Cl^+, but we will show in Part C that this contribution is negligible.) We therefore fit the Cl^+ angular distribution to a linear combination of the calculated CF_2Cl and Cl angular distributions, as shown in Fig. 5. At $\theta = 5°$, 40% of the Cl^+ signal comes from CF_2Cl. At larger angles, this percentage decreases, since the angular distribution of CF_2Cl is much narrower than that of Cl. This follows because the CF_2Cl product must be slower than Cl to conserve linear momentum. The same relative contributions of CF_2Cl and Cl which were used to fit the Cl^+ angular distribution also give good fits to the Cl^+ velocity distributions (see Fig. 6).

B. $CF_2Cl_2 \rightarrow CF_2 + Cl_2$

The velocity distributions of Cl_2^+ are shown in Fig. 7. At $\theta = 5°$, the Cl_2 product has a peak laboratory velocity nearly twice that of the CF_2Cl_2 molecular beam, confirming the presence of an exit barrier for this reaction. Since the products interact strongly as they descend this barrier, RRKM theory cannot be called upon to predict the product translational energy distribution (at least, not without additional assumptions). Instead, we tried to fit the experimental data with a translational energy distribution of the form $P(E) = (E-a)^2\exp(-E/b)$, treating a and b as adjustable parameters. Three such distributions are shown in Fig. 8. All three have a mean translational energy of 8 kcal/mole. In Fig. 7, the Cl_2 velocity distributions calculated from

these P(E)'s are compared with experiment. The P(E) represented by the solid curve in Fig. 8 gives the best fit to the data. This P(E) has a FWHM energy spread of 7.8 kcal/mole.

The present results on Cl_2 elimination from CF_2Cl_2 are remarkably similar to previous molecular beam results on HCl elimination from CF_2HCl.[8] In both cases the products are formed with a mean translational energy of 8 kcal/mole. The shapes of the P(E)'s are also very similar. This suggests that the character of the potential energy surface along the reaction coordinate is not very different for these two reactions. The height of the exit barrier for the HCl elimination reaction is known to be around 7 kcal/mole.[9] If we assume an identical barrier height for the reaction $CF_2Cl_2 \rightarrow CF_2 + Cl_2$, then the threshold for Cl_2 elimination is around 80 kcal/mole.

C. Secondary Dissociation of CF_2Cl

In Part A, we inferred that the CF_2Cl photofragments are formed with an averge internal energy of ~6.6 kcal/mole. The density of states of CF_2Cl at this level of excitation is extremely low. In addition, the nearest absorption band of CF_2Cl lies 65 cm^{-1} to the blue of the laser frequency used in our experiments.[10] Therefore, it seems very unlikely that the primary CF_2Cl products could themselves absorb photons from the laser field and dissociate.

Nevertheless, let us suppose for the moment that there is some secondary dissociation of CF_2Cl:

(3) $CF_2Cl \longrightarrow CF_2 + Cl$ $\quad \Delta H = 51$ kcal/mole.

Then the angular distributions and TOF spectra of CF_2^+ (and CF^+) must deviate from those of CF_2Cl^+ and $CFCl^+$, since additional translational energy is released in the secondary dissociation. Experimentally, the CF_2^+ and CF_2Cl^+ data are superimposable within experimental error. Of course, this does not prove that there is no secondary dissociation, but it is possible to put an upper bound on the percentage of secondary dissociation which may be occurring (at an energy fluence of 6 J/cm^2).

Before proceeding, we should first address the question of why the CF_2 radicals produced in the Cl_2 elimination reaction do not significantly perturb the measured angular and velocity distributions of CF_2^+, which are essentially identical to those of CF_2Cl^+. The answer has more to do with the kinematics than with the fact that Cl_2 elimination is a minor reaction channel. The CF_2Cl products are produced with relatively low kinetic energy and are scattered into a relatively narrow laboratory angular range. The CF_2 products from the elimination of Cl_2 are produced with much greater average kinetic energy and are scattered almost isotropically in the lab coordinate system. Therefore, at small lab angles ($\theta < 35^\circ$), only a very small fraction of the CF_2 products arising from Cl_2 elimination will get scattered into the solid angle viewed by the detector. Using the method to be described in Part D, we actually calculated that the contribution to the CF_2^+

signal from CF_2 is 440, 88 and 11 times smaller than the contribution from CF_2Cl at $\theta = 5^\circ$, 20° and 35°, respectively. Since the experimental error bars increase from 2% at $\theta = 5^\circ$ to 20% at $\theta = 35^\circ$, it is not surprising that this CF_2 contribution goes unnoticed.

Now back to the question of secondary dissociation. The sensitivity of the CF_2^+ angular distribution to any CF_2 produced via reaction (3) depends strongly on the amount of translational energy released in the secondary reaction. To estimate this translational energy, we proceeded as follows. The RRKM rate constant for reaction (3) increases so rapidly with excess energy that none of the CF_2Cl radicals are expected to absorb additional photons once they cross the dissociation threshold. We therefore assumed an average excess energy of 1.6 kcal/mole (0.5 photons) and used RRKM theory to calculate the product translational energy distribution. The mean CF_2 + Cl translational energy was 0.6 kcal/mole. The angular distribution of CF_2 (assuming complete secondary dissociation of CF_2Cl) was then calculated using this P(E) and the CF_2Cl laboratory angular and velocity distributions. In Fig. 9 this calculated distribution (short-dashed curve) is compared to the measured CF_2^+ angular distribution. The solid curve is the best fit to the CF_2Cl^+ angular distribution (see Fig. 2). In order to see what the CF_2^+ angular distribution would have looked like if an arbitrary percentage of the CF_2Cl product underwent secondary dissociation, an appropriate linear combination of the solid and dashed curves must be calculated, taking into account the slightly different probabilities of

detecting CF_2 and CF_2Cl radicals as CF_2^+ in the mass spectrometer. The long-dashed curve in Fig. 9 was calculated in this way, assuming 20% secondary dissociation. Given the size of the experimental error bars, we regard this figure as a conservative upper bound on the extent of seconday dissociation which may be occurring at an energy fluence of 6 J/cm^2.

D. Branching Ratio

We define the branching ratio R to be the ratio of the fraction of molecules dissociating through the Cl_2 elimination channel (x_{Cl_2}) to the fraction of molecules dissociating through the Cl elimination channel ($1-x_{Cl_2}$):

$$R = \frac{x_{Cl_2}}{1 - x_{Cl_2}} .$$

(We are assuming that all molecules which dissociate follow one of these two channels.)

The experimental determination of R involves two distinct steps. First, we need to calculate the true product signals from the ion signals measured in the mass spectrometer. Second, we need to transform these product signals from the LAB to the CM system. We will discuss these two steps in detail below.

With the detector at $\theta = 5^{\circ}$, we set the quadrupole mass filter to near unit mass resolution and compared the mass spectrometer signals at m/e = 70 ($^{35,35}Cl_2^+$) and at m/e = 66 ($CF^{35}Cl^+$). We obtained 0.036 ion counts/laser pulse at m/e = 70 and 1.39 counts/pulse at m/e = 66. After correcting for isotopic abundance, this yields a Cl_2^+ to $CFCl^+$ ratio of

$$\frac{N_{Cl_2^+}\ (5^{\circ})}{N_{CFCl^+}\ (5^{\circ})} = 0.034.$$

In order to relate these ion signals to the Cl_2 and CF_2Cl product signals, we have to understand the nature of the electron bombardment ionization process. Consider the electron bombardment ionization of a molecule or radical P. The initial ionization event involves the formation of the parent molecular ion,

$$e + P \longrightarrow P^+ + 2\ e.$$

The probability of this event is proportional to the total ionization cross section of P, σ_{ion} (P). If the parent ion is formed with sufficient internal excitation, it may unimolecularly decompose to produce a variety of daughter ions,

$$P^+ \longrightarrow D_i^+ \qquad i = 1, 2, \ldots$$

The fraction of the parent ions P^+ which fragment to give the daughter ion D_i^+ will be denoted by $f(D_i^+ \mid P)$.

Therefore, the measured Cl_2^+:$CFCl^+$ ion signal ratio is related to the true Cl_2:CF_2Cl product ratio according to

$$\frac{N_{Cl_2^+}(5°)}{N_{CFCl^+}(5°)} = \frac{N_{Cl_2}(5°) \cdot \sigma_{ion}(Cl_2) \cdot f(Cl_2^+ \mid Cl_2)}{N_{CF_2Cl}(5°) \cdot \sigma_{ion}(CF_2Cl) \cdot f(CFCl^+ \mid CF_2Cl)} .$$

In general, when comparing two ion signals, one must also consider differences in the transmission of the quadrupole mass spectrometer, but this effect is negligible in the present case due to the similar masses of Cl_2^+ and $CFCl^+$.

The relative ionization cross sections of Cl_2 and CF_2Cl were estimated as follows. Center and Mandl[11] have shown that, for a wide variety of atomic and molecular species, a good correlation exists between the maximum ionization cross section and the square root of the polarizability. From Fig. 2 of Ref. 11 we obtain the relation

$$\sigma_{ion} = 36\sqrt{\alpha} - 18,$$

where σ_{ion} is the maximum ionization cross section in units of $Å^2$ and α is the polarizability in $Å^3$. Our ionizer was operated at an electron energy of 200 eV, which is close to the maximum of the ionization cross section curve for most species. We took the molecular polarizability to be the sum of the atomic polarizabilities. Values of atomic polarizabilities were taken from the review article by Miller and Bederson:[12] $\alpha_C = 1.76$, $\alpha_F = 0.557$, $\alpha_{Cl} = 2.18$, all in units of

$Å^3$. We obtain

$$\frac{\sigma_{ion}\,(Cl_2)}{\sigma_{ion}\,(CF_2Cl)} = \frac{57.2}{62.9} = 0.91.$$

The fragmentation pattern of CF_2Cl was measured at $\theta = 5°$. The major daughter ions and their weights relative to CF_2Cl^+ are listed below:

$$CF_2Cl^+:CFCl^+:CF_2^+:CF^+:Cl^+ = 100:35:82:52:29.$$

For these measurements the quadrupole resolution was set very low to allow collection of both Cl isotopes and to minimize differences in ion transmission. The Cl^+ signal was corrected for the contribution from Cl atoms as described in Part A. The estimated contributions to the CF_2^+, CF^+ and Cl^+ signals from CF_2 and Cl_2 were very small and were ignored. We conclude that 12% of the CF_2Cl radicals which are ionized fragment to give $CFCl^+$, i.e., $f(CFCl^+|CF_2Cl) = 0.12$. The Cl_2 fragmentation pattern was determined by pointing the detector directly into a beam of Cl_2. The ratio of Cl_2^+ to Cl^+ was 8.5:1. Therefore $f(Cl_2^+|Cl_2) = 0.90$.

We can now calculate the Cl_2:CF_2Cl product ratio at $\theta = 5°$.

$$\frac{N_{Cl_2}\,(5°)}{N_{CF_2Cl}\,(5°)} = \frac{N_{Cl_2^+}\,(5°)}{N_{CFCl^+}\,(5°)} \cdot \frac{\sigma_{ion}\,(CF_2Cl)}{\sigma_{ion}\,(Cl_2)} \cdot \frac{f(CFCl^+|CF_2Cl)}{f(Cl_2^+|Cl_2)}$$

$$= (0.034) \cdot \left(\frac{1}{0.91}\right) \cdot \left(\frac{0.12}{0.90}\right)$$

$$= 0.0050.$$

Now we have to transform this LAB quantity to the CM system. Using the known CM translational energy distributions for reactions (1) and (2), it is easy to calculate the laboratory Cl_2:CF_2Cl product ratio at θ = 5° as a function of the branching ratio R. The details of the general procedure are given in Appendix II. The result is

$$\frac{N_{Cl_2}(5°)}{N_{CF_2Cl}(5°)} = 0.0416 \cdot R .$$

We conclude that

$$R = 0.120$$

and

$$x_{Cl_2} = 0.107.$$

Therefore, about 10% of the CF_2Cl_2 molecules which dissociate yield $CF_2 + Cl_2$ at an energy fluence of 6 J/cm^2.

To check the reliability of this procedure of relating LAB ion signals to CM product fluxes, we also compared the experimental and theoretical CF_2Cl:Cl ratio at various lab angles. Since CF_2Cl and Cl come from the same dissociation channel, the CF_2Cl:Cl ratio in the CM frame is one, and the theoretical CF_2Cl:Cl ratio at any lab angle will depend only on the CM translational energy distribution for this channel, the molecular beam velocity, and conservation of linear momentum.

The experimental CF_2Cl:Cl ratio at $\theta = 5^\circ$ (obtained by correcting the measured ion signals as described above) was 3.99. The theoretical ratio at this angle, calculated using the best-fit P(E), was 3.96. Agreement this good is, of course, just an accident. Still, it reassures us that our determinations of fragmentation patterns and relative ionization cross sections are not grossly in error.

Finally, the dependence of the branching ratio on energy fluence was investigated over the range 0.3-8 J/cm^2. (Since the pulse length is constant, the energy fluence is proportional to the laser intensity.) For these measurements, CF_2Cl^+ and Cl_2^+ were monitored at $\theta = 10^\circ$. Also, in order to reduce counting times, the quadrupole resolution was lowered to ~3 amu FWHM so that both $CF_2{}^{35}Cl^+$ and $CF_2{}^{37}Cl^+$ as well as $^{35,35}Cl_2^+$ and $^{35,37}Cl_2^+$ could be counted. Even at this lower resolution, there was very little contamination of the Cl_2^+ signal by $CF^{37}Cl^+$, since the different TOF spectra of Cl_2 and CF_2Cl allowed us to discriminate against CF_2Cl when counting Cl_2 (see Fig. 1). The branching ratios were calculated in the manner described previously, assuming now that all Cl isotopes were detected. The results are shown in Fig. 10, together with the single point derived earlier by comparing the $^{35,35}Cl_2^+$ and $CF^{35}Cl^+$ signal at $\theta = 5^\circ$. It appears that the branching ratio may shift slightly in favor of the Cl elimination channel as the energy fluence is increased.

IV. DISCUSSION

A. Product Energy Distributions

$CF_2Cl_2 \rightarrow CF_2Cl + Cl$

Our results on the Cl elimination reaction are generally in good agreement with the earlier results of Sudbo et al.,[1] although the present results are more precise. There is, however, one minor discrepancy. Sudbo et al. claimed that the Cl^+ signal was correctly related to the CF_2Cl^+ signal by momentum conservation and concluded that the Cl^+ signal originated from Cl with little contribution from fragmentation of CF_2Cl in the ionizer. In fact, Cl^+ is one of the major ions in the mass spectrum of the CF_2Cl radical, and at $\theta = 5°$ almost half of the Cl^+ signal arises from CF_2Cl.

The fact that the $CF_2Cl + Cl$ translational energy distribution is well described by RRKM theory does not in itself constitute proof that the reaction proceeds statistically. The shape of the translational energy distribution is really not too sensitive to the extent of energy randomization. This point has been emphasized recently by Thiele, Goodman and Stone.[13] However, the general conclusion that RRKM theory correctly describes infrared multiphoton dissociation processes is not based on the shape of the translational energy distribution alone. Rather, it is based on the consistency of a large number of experimental observations covering a wide variety of polyatomic molecules. The evidence is particularly compelling in the case of SF_6, for which experimental data exists on the average level of molecular excitation and the phenomenological absorption cross section (from optoacoustic measurements[14]), the average

dissociation lifetime (from observation of secondary dissociation of SF_5 during the CO_2 laser pulse[15]), and the SF_5 + F product translational energy distribution,[15] all as a function of the laser intensity and energy fluence. The data agree nicely with the predictions of a very simple rate equation model which assumes, for molecules above the dissociation threshold, a competition between the intensity-dependent excitation rate and the rate of statistical unimolecular reaction.

Although we do not have independent data on the average level of excitation or the dissociation lifetime in the case of CF_2Cl_2, we will assume for now that the Cl elimination reaction is in fact statistical. Then, as discussed in Sec. III A, we can infer that the average level of molecular excitation is ~8 kcal/mole beyond the C-Cl dissociation threshold and that the unimolecular rate constant for the Cl elimination reaction is around 2.5×10^8 sec^{-1}. In Part B of this Discussion, we will follow through the consequences of this assumption when we compare the experimental and RRKM theoretical branching ratios at this predicted average level of excitation.

We have assumed a "loose" critical configuration in the RRKM calculation for the Cl elimination reaction. That is, the two bending frequencies associated with the departing Cl atom have been substantially lowered in the critical configuration (compared to the same frequencies in the molecule). Our particular choices for these frequencies are, of course, somewhat arbitrary. We should point out, though, that while the rate constant is quite sensitive to the specific choices for the critical configuration frequencies, the translational energy distribution is

extremely insensitive to these choices. This is because the problem of determining the fraction, f, of the excess energy which enters translation (i.e., the reaction coordinate) is really just a problem in equipartition of energy. For low excess energies, f will depend somewhat on the frequencies (by way of the vibrational partition function), since higher frequency vibrations may be "frozen" at low energies. However, for sufficiently high excess energies, f has to converge to the classical equipartition result, $1/(3N-6)$, where N is the number of atoms in the molecule. For CF_2Cl_2, $N = 5$ and $1/(3N-6) = 0.11$. The RRKM calculation gives $f = 1.4/7.8 = 0.18$ for an excess energy of 7.8 kcal/mole. Therefore at this relatively low excess energy the translational degree of freedom is getting a little more than its classical "fair-share", mainly at the expense of the high-frequency C-F stretching vibrations.

$CF_2Cl_2 \rightarrow CF_2 + Cl_2$

Our determination of the product translational energy distribution for the Cl_2 elimination reaction is incompatible with the estimates of Stephenson and King[3] (hereafter abbreviated SK). We find that the CF_2 fragments are formed with an average translational energy of 4.7 ± 0.3 kcal/mole, compared to SK's estimate of 1.5 ± 0.5 kcal/mole. In addition to CF_2Cl_2, SK have also studied CF_2Br_2,[3] CF_2HCl[3] and CF_2CFCl.[16] Since molecular beam data exists only for CF_2Cl_2 and CF_2HCl, we will concentrate on these two molecules in our discussion.

In SK's experiment, infrared pulses from a CO_2 TEA laser and ultraviolet pulses from a frequency doubled N_2-pumped dye laser were

propagated anti-colinearly down the center of a gas cell containing low pressures (< 8 mtorr) of CF_2Cl_2 or CF_2HCl. The radius of the IR beam was 0.047 cm, while the radius of the UV beam was 0.005 cm. The CF_2 fragments were initially generated in a well-defined cylindrical region. The concentration of CF_2 along the axis of this cylinder was then probed by UV laser-induced fluorescence as a function of the delay time between the start of the CO_2 laser pulse and the UV pulse. Assuming a Boltzmann velocity distribution for the CF_2 products, SK show that for long times after the CO_2 laser pulse the laser-induced fluorescence intensity, S(t), should fall off with a $1/t^2$ time-dependence. The slope of a plot of S(t) vs. $1/t^2$ is related to the most probable velocity of the Boltzmann distribution, from which the average translational energy, E_T, may be calculated. SK confirmed that $S(t) \propto 1/t^2$ for delay times greater than 1-2 μs. They calculated average translational energies of 1.5 ± 0.5 kcal/mole and 6.9 ± 2 kcal/mole for the CF_2 produced from CF_2Cl_2 and CF_2HCl, respectively. Compared to the molecular beam results, SK's value for E_T (CF_2) is three times too low in the case of CF_2Cl_2, and two times too high in the case of CF_2HCl. In fact, the molecular beam results show that the product translational energy distributions are nearly identical for $CF_2Cl_2 \rightarrow CF_2 + Cl_2$ and for $CF_2HCl \rightarrow CF_2 + HCl$. The differences in the CF_2 velocity and energy distributions are slight, due only to the different product mass combinations. Why, then, do SK's results differ so dramatically for these apparently very similar reactions?

In the Appendix to Ref. 3, SK suggest that if the product velocity distribution is closer to a delta function than to a Boltzmann distribution, then their E_T values would be lower by a factor of two. While this would improve the agreement in the case of CF_2HCl, it would make matters even worse for CF_2Cl_2. As mentioned in the introduction, another possibility is that most of the CF_2 produced from CF_2Cl_2 is coming from secondary dissociation of CF_2Cl. (Such complications cannot arise for CF_2HCl, since HCl elimination is the only important dissociation channel.) While SK initially argued against this possibility,[2] more recently they have suggested[17] that secondary dissociation is actually the dominant source of CF_2. Although we saw no positive evidence for secondary dissociation in the present experiment, we are, unfortunately, not very sensitive to this process.

However, even in the absence of such interference, SK's optical TOF technique may run into trouble because it has a strong bias for the products formed with low translational energy. With a minimum delay time of 1 μs and an IR beam radius of 0.05 cm, the detected products will mainly have speeds slower than 5×10^4 cm/sec. From the present experiment and Ref. 8, we know that the most probable velocities of the CF_2 produced from CF_2Cl_2 and CF_2HCl are 7.4×10^4 cm/sec and 6.1×10^4 cm/sec, respectively. Also, the distribution of recoil velocities is rather sharply peaked about the most probable value for both of these reactions. Consequently, most of the CF_2 radicals have already left the cylindrical viewing region before SK commence their

measurements. Only the slower products are left behind to be detected. If the product velocity distribution is actually close to Boltzmann, then SK's experiment could still yield the correct value for the most probable velocity. However, if the distribution is much different from Boltzmann, then it is impossible to find the most probable velocity by just looking at the slow end of the velocity distribution. It appears that the utility of this optical TOF method is severely limited unless the shape of the product velocity distribution is accurately known beforehand.

The above observations may also be relevant to one other aspect of SK's results which we find puzzling. In the case of CF_2HCl, SK claim that the average translational energy is the same for CF_2 ($v = 0$) and CF_2 ($\nu_2 = 5$), the latter of which contains 3320 cm^{-1} of vibrational energy, which is the equivalent of ~3 CO_2 laser photons. Since the RRKM rate constant for CF_2HCl increases by more than a factor of six for each additional photon absorbed beyond the dissociation threshold, it seems unlikely that the spread of excess energy of the molecules which dissociate is much more than one or two photons. Therefore, while the population distribution in the quasicontinuum is expected to be close to thermal, the distribution of the molecules which dissociate is probably closer to a microcanonical ensemble (characterized by an energy E*) than to a canonical ensemble (characterized by a temperature T). In a microcanonical ensemble, energy must be conserved. Therefore, if a large amount of energy enters product vibration, we would expect to see a smaller amount of energy in product translation and/or rotation, and vice versa. In particular, the translational energy distribution of CF_2

(v = 0) should be skewed to higher energies than that for CF_2 (ν_2 = 5). The fact that SK observe essentially identical diffusional profiles for CF_2 (v = 0) and CF_2 (ν_2 = 5) may indicate not that the average translational energies are the same, but rather that the slow ends of the CF_2 (v = 0) and CF_2 (ν_2 = 5) velocity distributions are very similar.

B. Experimental and RRKM Branching Ratios.

Our result for the Cl_2:Cl branching ratio at 6 J/cm^2 is R = 0.120. This ratio changes by less than 25% over the fluence range 0.5 - 8 J/cm^2. Hudgens[4] obtained R < 0.03 for fluences between 10 and 140 J/cm^2. As mentioned in the introduction, Hudgens obtained this estimate by comparing the $^{35}Cl^+$ and $^{35,35}Cl_2^+$ signals in his beam sampling mass spectrometer following a CO_2 laser pulse. Although Hudgens corrected for isotopic abundances, relative ionization cross sections and Cl_2 fragmentation in the ionizer, there are several other important factors for which he apparently did not (or could not) correct. First, the differing kinematics of the two reactions were not taken into account. The mass spectrometer, which looks directly into the CF_2Cl_2 gas flow, is more sensitive to the slower products of the Cl elimination reaction, since they are scattered into a narrower angular range than the products of the molecular elimination reaction. Second, the ion signals were not corrected for the 1/v velocity dependence of the ionization probability. Since the average velocity of the Cl_2 products is significantly higher than for the CF_2Cl and Cl products, this correction

would tend to increase the measured Cl_2 signal relative to Cl. Third, the Cl^+ signal was not corrected for contributions from CF_2Cl. Therefore the measured Cl^+ signal overestimates the true Cl signal. All three of these factors would tend to increase Hudgens' value for R, presumably bringing it closer to our result.

We now wish to consider our experimental branching ratio in the context of RRKM theory. The microcanonical RRKM branching ratio is, of course, only a function of the excitation energy E*:

$$R(E^*) = \frac{1}{2} \frac{G_{Cl_2}(E^\dagger_{Cl_2} = E^* - E^0_{Cl_2})}{G_{Cl}(E^\dagger_{Cl} = E^* - E^0_{Cl})} \quad .$$

E^0_{Cl} is the energy threshold, $E^\dagger_{Cl}$ is the excess energy, and G_{Cl} $(E^\dagger_{Cl})$ is the total number of internal states available to the critical configuration for the Cl elimination reaction. $E^0_{Cl_2}$, $E^\dagger_{Cl_2}$ and G_{Cl_2} $(E^\dagger_{Cl_2})$ are the corresponding quantities for the Cl_2 elimination reaction. The factor of 1/2 enters because the reaction path degeneracy is two for the Cl elimination reaction.

The relevant energetics are depicted in Fig. 11. The enthalpy change for the Cl_2 elimination reaction was calculated using ΔH^0_f $(CF_2Cl_2) = -117.5 \pm 2$ kcal/mole[18] and ΔH^0_f $(CF_2) = -44.5 \pm 0.4$ kcal/mole.[19] The energy threshold for this reaction is assumed to be 7 kcal/mole higher than the endothermicity, by analogy with the $CF_2HCl \rightarrow CF_2 + HCl$ reaction.[9] (For CF_2, unlike CH_2, the ground electronic state is the singlet, with the lowest triplet state lying 47 kcal/mole higher in energy.[20] Therefore CF_2Cl_2 can adiabatically dissociate

to give ground electronic state CF_2 and Cl_2 products.) Unfortunately, the heat of formation of the CF_2Cl radical is not known. However, Foon and Tait[21] have estimated the dissociation energy D(R-Cl) for CF_3Cl, CF_2Cl_2, $CFCl_3$, and CCl_4 using a competitive kinetic technique (see Table 1). Their results reveal the interesting trend that the R-Cl bond strength increases as fluorine is substituted for chlorine. While this trend in bond strengths is expected to be fairly reliable (since similar assumptions were made for each member of the homologous series), the absolute values for $D(CF_3-Cl)$ and $D(CCl_3-Cl)$ are 3-5 kcal/mole lower than the values calculated using accurate JANAF[18] data. This suggests that the other two bond strengths are also too low by about the same amount. We therefore increased $D(CF_2Cl-Cl)$ from 76 kcal/mole to 80 kcal/mole. (The resulting value for ΔH_f^0 (CF_2Cl) is -66.5 kcal/mole. This was used earlier to calculate the CF_2-Cl bond energy.) In summary, the energy thresholds for Cl and Cl_2 elimination appear to be essentially identical, although when the uncertainties are taken into account the energy separation could go several kcal/mole in either direction. As we shall see, for a small molecule like CF_2Cl_2, the RRKM branching ratio depends critically on the value of this energy separation.

In most applications of RRKM theory, the high-pressure Arrhenius A-factor is used to constrain the model for the critical configuration. It is well known that the calculated k(E*) vs. E* curve is extremely insensitive to the exact choices of the critical configuration parameters, so long as these parameters are chosen to reproduce the experimental

A-factor (see Ch. 6 of Ref. 22). Although A-factors have not been measured for the reactions considered here, we can still hope to come up with reasonable models of the critical configurations for the Cl and Cl_2 elimination reactions by considering results on similar systems. It is clear that the Cl elimination reaction, like other simple bond fission reactions, should be modeled by a "loose" critical configuration, where the bending frequencies associated with the C-Cl bond being broken are substantially lowered in the critical configuration compared to the same frequencies in the excited molecule. (Typical range for A-factors of simple fission reactions: $\log_{10}A$ = 14-16.) On the other hand, the Cl_2 elimination reaction is expected to proceed through a "tighter" critical configuration with frequencies not much different from those in the molecule. (Typical range for A-factors of 3-center elimination reactions: $\log_{10}A$ = 12-14.) In Appendix I, we have calculated the RRKM rate constant vs. excess energy curves for both reactions assuming fairly "loose" and "tight" critical configurations for the Cl and Cl_2 eliminations, respectively. The models we have chosen for the critical configurations yield high-pressure A-factors of $\log_{10}A$ = 15.4 for the Cl elimination reaction and $\log_{10}A$ = 13.4 for the Cl_2 elimination reaction at a temperature of 1000°K. If the energy thresholds for the two reactions are equal, the predicted branching ratio is 0.030 at an excess energy of 8.0 kcal/mole, which is about three times lower than the experimental result. Also, for equal thresholds, the RRKM branching ratio changes very slowly with excess energy, decreasing from R = 0.035 at $E^\dagger$ = 1.8 kcal/mole to R = 0.029 at $E^\dagger$ = 15.5 kcal/mole. That is, the curvature

of the k(E*) vs. E* curve is only slightly greater for the Cl_2 elimination reaction than for the Cl elimination reaction. The two curves in Fig. A1 are mainly just displaced vertically by a factor of ~30. This contrasts with the results shown in Fig. 5 of Ref. 23. We were unable to reproduce the k_{Cl_2} (E*) vs. E* curve of Grant et al.[23] for any values of the critical configuration frequencies. Apparently, their curve was determined empirically to fit their data, and is not the result of an RRKM calculation.

The agreement between the experimental and RRKM branching ratios could be improved by either making $E^0_{Cl_2}$ somewhat lower than E^0_{Cl} (the agreement is exact if $E^0_{Cl_2}$ is 4 kcal/mole lower than E^0_{Cl}) or by lowering some of the frequencies in the critical configuration of the Cl_2 elimination reaction. However, it should be emphasized that if $E^0_{Cl_2}$ were to lie much more than 4 kcal/mole below E^0_{Cl}, it would be impossible to obtain an RRKM branching ratio of 0.1 without resorting to unreasonable critical configuration parameters.

Even if $E^0_{Cl_2}$ lies above E^0_{Cl}, it may be possible for RRKM theory to reproduce the observed branching ratio. In this case, it is necessary to further loosen the Cl_2 critical configuration. If identical critical configuration frequencies are chosen for both reactions, then the RRKM branching ratio agrees with experiment if $E^0_{Cl_2}$ lies 4 kcal/mole above E^0_{Cl}. It is impossible to obtain agreement if $E^0_{Cl_2}$ lies more than 4 kcal/mole above E^0_{Cl}, unless we allow the concerted Cl_2 elimination reaction to proceed through a <u>looser</u> critical configuration than the Cl elimination reaction. This is

an extreme assumption, not at all reasonable, and the value $E^0_{Cl_2} - E^0_{Cl} = 4$ kcal/mole should be considered as an upper bound. In addition, if $E^0_{Cl_2}$ lies significantly above E^0_{Cl}, the branching ratio must increase (shift in favor of Cl_2) as the energy is increased (at least this is true in the energy range of interest, 1-15 kcal/mole above E^0_{Cl}). This would seem to contradict the experimental result that R remains constant, or decreases slightly, as the laser intensity is increased. Since the error bars in Fig. 9 are rather large, and since we probably are not changing the excitation energy too much as we vary the laser intensity over one decade, we cannot rule out the possibility that $E^0_{Cl_2}$ lies somewhat above E^0_{Cl}. However, we disagree with the contention of Grant et al.[5,23] that the branching ratio at the level of excitation under consideration can shift in favor of the atomic elimination as the excitation energy is increased even if $E^0_{Cl_2}$ lies above E^0_{Cl}.

To summarize, we have shown that one may reasonably obtain agreement between the experimental and RRKM branching ratios only if the energy threshold separation, $\left|E^0_{Cl_2} - E^0_{Cl}\right|$, is less than 4 kcal/mole. The true energy threshold separation, estimated to be $E^0_{Cl_2} - E^0_{Cl} = 0 \pm 3$ kcal/mole, satisfies this constraint. Unfortunately, the experimental uncertainty in $E^0_{Cl_2} - E^0_{Cl}$ is rather large. Therefore any more detailed conclusions must await better thermochemical and/or kinetic data which would allow the energy threshold separation and critical configuration parameters to be specified more precisely.

ACKNOWLEDGMENTS

This work was supported by the Director, Office of Energy Research, Office of Basic Energy Sciences, Chemical Sciences Division and the Assistant Secretary for Nuclear Energy, Office of Advanced Systems and Nuclear Projects, Advanced Isotope Separation Division, U.S. Department of Energy under Contract Number DE-AC03-76SF00098. F. H. acknowledges a fellowship from the Max-Planck-Gesellschaft, Munchen, Federal Republic of Germany.

REFERENCES

a. Also associated with the Department of Chemistry, University of California, Berkeley, California 94720.

b. Permanent address: Max-Planck-Institut fur Stromungsforschung, D-3400 Gottingen, Federal Republic of Germany.

c. Permanent address: Physics Department, Fudan University, Shanghai, People's Republic of China.

d. Also associated with the Department of Physics, University of California, Berkeley, California 94720.

e. Miller Professor, 1981-1982.

1. Aa. S. Sudbo, P. A. Schulz, E. R. Grant, Y. R. Shen and Y. T. Lee, J. Chem. Phys. 70, 912 (1979).

2. D. S. King and J. C. Stephenson, Chem. Phys. Lett. 51, 48 (1977).

3. J. C. Stephenson and D. S. King, J. Chem. Phys. 69, 1485 (1978).

4. J. W. Hudgens, J. Chem. Phys. 68, 777 (1978).

5. R. J. S. Morrison and E. R. Grant, J. Chem. Phys. 71, 3537 (1979).

6. Y. T. Lee, J. D. McDonald, P. R. LeBreton and D. R. Herschbach, Rev. Sci. Instrum. 40, 1402 (1969).

7. L. H. Ngai and R. H. Mann, J. Mol. Spectrosc. 38, 322 (1971).

8. Aa. S. Sudbo, P. A. Schulz, Y. R. Shen and Y. T. Lee, J. Chem. Phys. 69, 2312 (1978).

9. J. W. Edwards and P. A. Small, Ind. Eng. Chem. Fundam. 4, 396 (1965). Edwards and Small report an activation energy of 55.8 kcal/mole for the reaction $CF_2HCl \rightarrow CF_2 + HCl$. Using this value together with ΔH_f^0 (CF_2HCl) = -115.1 kcal/mole (JANAF),

ΔH_f^0 (HCl) = -22.1 kcal/mole (JANAF), and ΔH_f^0 (CF_2) = -44.5 kcal/mole (Ref. 19) yields a barrier height of 7.3 kcal/mole for HCl addition to CF_2.

10. D. E. Milligan, M. E. Jacox, J. H. McAuley and C. E. Smith, J. Mol. Spectrosc. 45, 377 (1973).
11. R. E. Center and A. Mandl, J. Chem. Phys. 57, 4104 (1972).
12. T. M. Miller and B. Bederson, Adv. At. Mol. Phys. 13, 1 (1977).
13. E. Thiele, M. F. Goodman and J. Stone, Chem. Phys. Lett. 69, 18 (1980).
14. J. G. Black, P. Kolodner, M. J. Shultz, E. Yablonovitch and N. Bloembergen, Phys. Rev. A19, 704 (1979).
15. P. A. Schulz, Aa. S. Sudbo, E. R. Grant, Y. R. Shen and Y. T. Lee, J. Chem. Phys. 72, 4985 (1980).
16. J. C. Stephenson, S. E. Bialkowski and D. S. King, J. Chem. Phys. 72, 1161 (1980).
17. See the discussion on p.1163 of Ref. 16.
18. JANAF Thermochemical Tables, 2nd ed., Natl. Stand. Ref. Data Ser., U.S. Natl. Bur. Stand. 37 (U.S. Government Printing Office, Washington, D.C., 1971).
19. G. A. Carlson, J. Phys. Chem. 75, 1625 (1971). We believe that this determination of ΔH_f^0 (CF_2) is the most accurate and precise, and prefer it to the JANAF recommended value.
20. V. Staemmler, Theor. Chim. Acta 35, 309 (1974).
21. R. Foon and K. B. Tait, J. Chem. Soc., Faraday Trans. 1, 68, 1121 (1972).

22. See, for example, P. J. Robinson and K. A. Holbrook, Unimolecular Reactions (Wiley, New York, 1972).

23. R. J. S. Morrison, R. F. Loring, R. L. Farley and E. R. Grant, J. Chem. Phys. 75, 148 (1981).

24. G. L. Catchen, J. Husain and R. N. Zare, J. Chem. Phys. 69, 1737 (1978).

Table 1. R-Cl Bond Dissociation Energies

Molecule	D(R - Cl) (kcal/mole)	
	Experimental (Ref. 21)	Calculated using JANAF data (Ref. 18)
CF_3Cl	81	86
CF_2Cl_2	76	--
$CFCl_3$	72	--
CCl_4	68	71

FIGURE CAPTIONS

Fig. 1. Time-of-flight distributions of CF_2Cl^+ and Cl_2^+ measured at $\theta = 5^\circ$. The distance from the interaction region to the center of the ionizer is 21.2 cm. The time scale has not been corrected for the flight time of the ions through the mass spectrometer (about 29 μs for CF_2Cl^+ and 26 μs for Cl_2^+).

Fig. 2. Laboratory angular distribution of CF_2Cl. O Experimental points (CF_2Cl^+ monitored by the mass spectrometer). Error bars represent two standard deviations. The curves were calculated from the P(E)'s shown in Fig. 4.

Fig. 3. Laboratory velocity flux distributions of CF_2Cl. Symbols as in Fig. 2.

Fig. 4. RRKM center-of-mass translational energy distributions for the products of the Cl elimination reaction.

——— ——— 3.3 kcal/mole excess energy;

——————— 8.0 kcal/mole excess energy;

- - - - - - - - - 12.6 kcal/mole excess energy.

Fig. 5. Angular distribution of Cl^+ mass spectrometer signal.

O Experimental points (error bars represent two standard deviations);

——————— Best fit, obtained by adding the individual contributions (dashed curves) of the Cl and CF_2Cl dissociation fragments to the Cl^+ signal. The dashed curves were calculated from the solid-line P(E) in Fig. 4.

Fig. 6. Velocity flux distributions of the Cl^+ mass spectrometer signal. Symbols as in Fig. 5.

Fig. 7. Velocity flux distributions of Cl_2. O Experimental points (Cl_2^+ monitored). The curves were calculated from the P(E)'s in Fig. 8.

Fig. 8. Trial center-of-mass translational energy distributions for the products of the Cl_2 elimination reaction.

$P(E) \propto (E - a)^2 \exp(-E/b)$

—— —— $a = 0$, $b = 8/3$;

———— $a = 1$, $b = 7/3$;

- - - - - $a = 2$, $b = 2$.

All three distributions have a mean translational energy of 8 kcal/mole.

Fig. 9. Angular distribution of CF_2^+ mass spectrometer signal.

O Experimental points (error bars represent two standard deviations);

———— Theoretical CF_2Cl angular distribution calculated from the solid-line P(E) in Fig. 4;

- - - - - Calculated CF_2^+ angular distribution assuming complete secondary dissociation of CF_2Cl;

—— —— Calculated CF_2^+ angular distribution assuming 20% secondary dissociation.

Fig. 10. Ratio of molecular to atomic chlorine elimination from CF_2Cl_2 vs. laser energy fluence.

● CF_2Cl^+ and Cl_2^+ monitored at $\theta = 10°$;

O $CFCl^+$ and Cl_2^+ monitored at $\theta = 5°$.

Error bars represent one standard deviation.

(Note offset vertical scale.)

Fig. 11. Energy diagram for CF_2Cl_2 dissociation. The average level of excitation of the molecules which dissociate is estimated to be 88 kcal/mole.

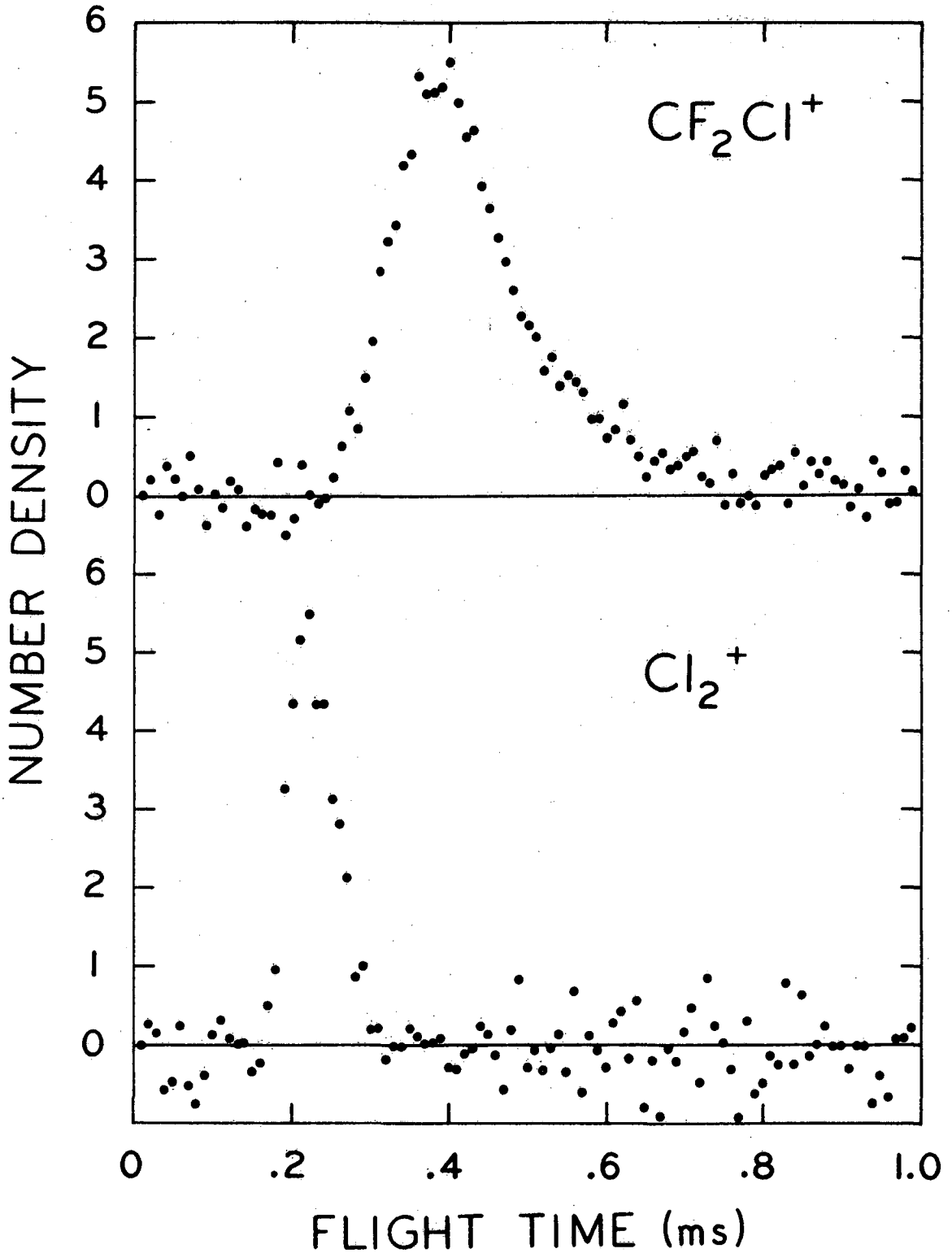

Fig. 1

XBL 814-9367

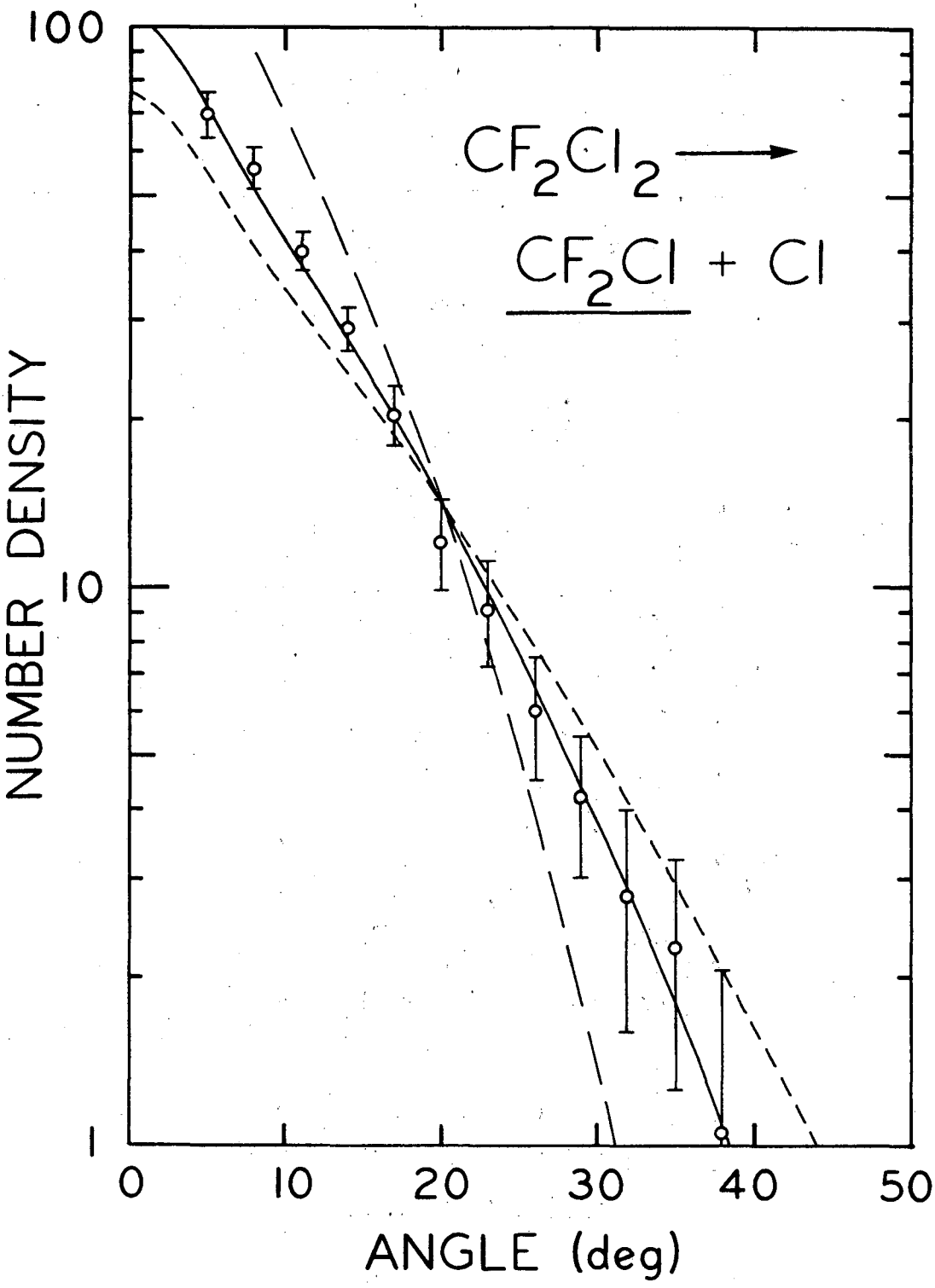

XBL 814-9359

Fig. 2

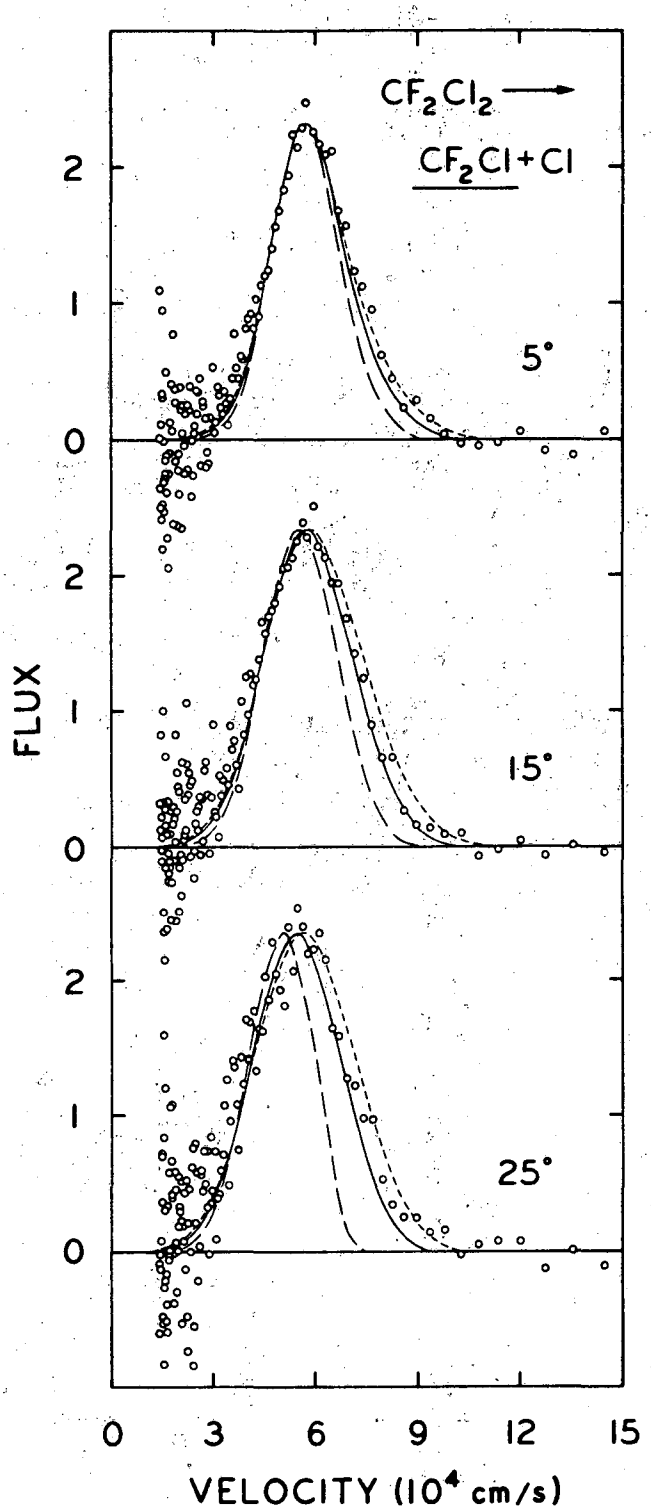
CF_2Cl_2 ⟶
CF_2Cl+Cl
5°
15°
25°
FLUX
VELOCITY (10^4 cm/s)
0
3
6
9
12
15
XBL 814-9368

Fig. 3

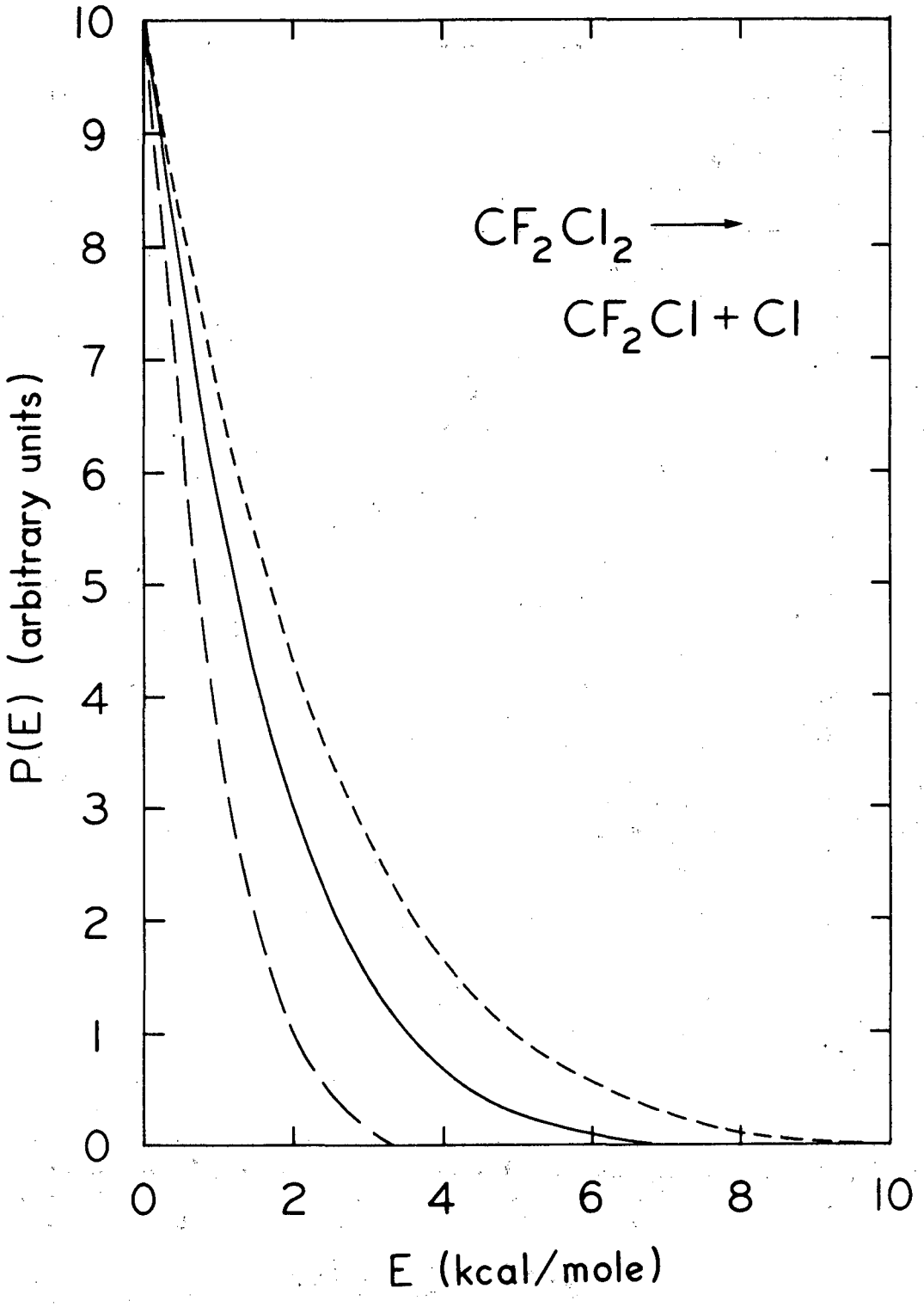

XBL 814-9365

Fig. 4

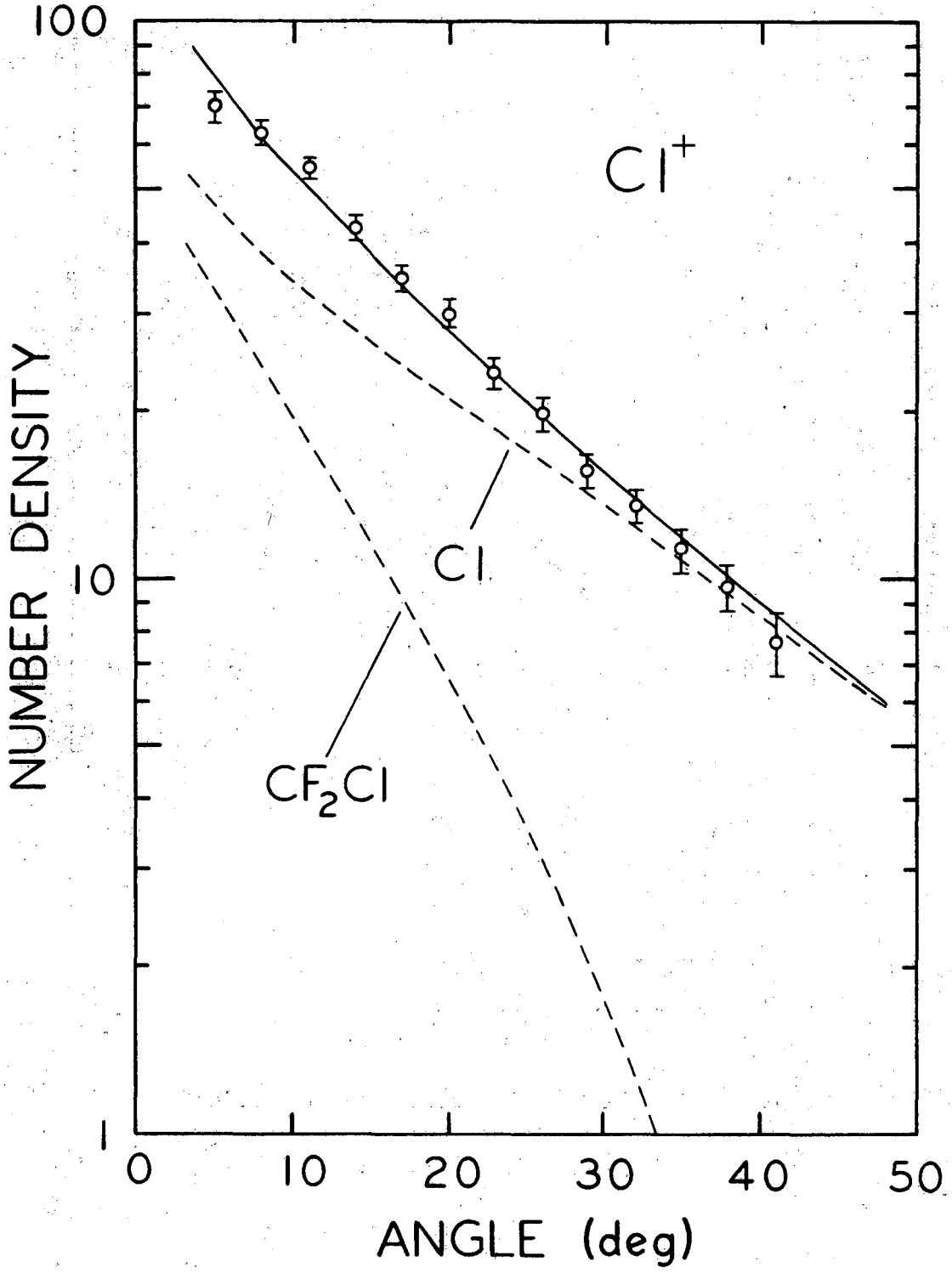

Fig. 5

XBL 814-9360

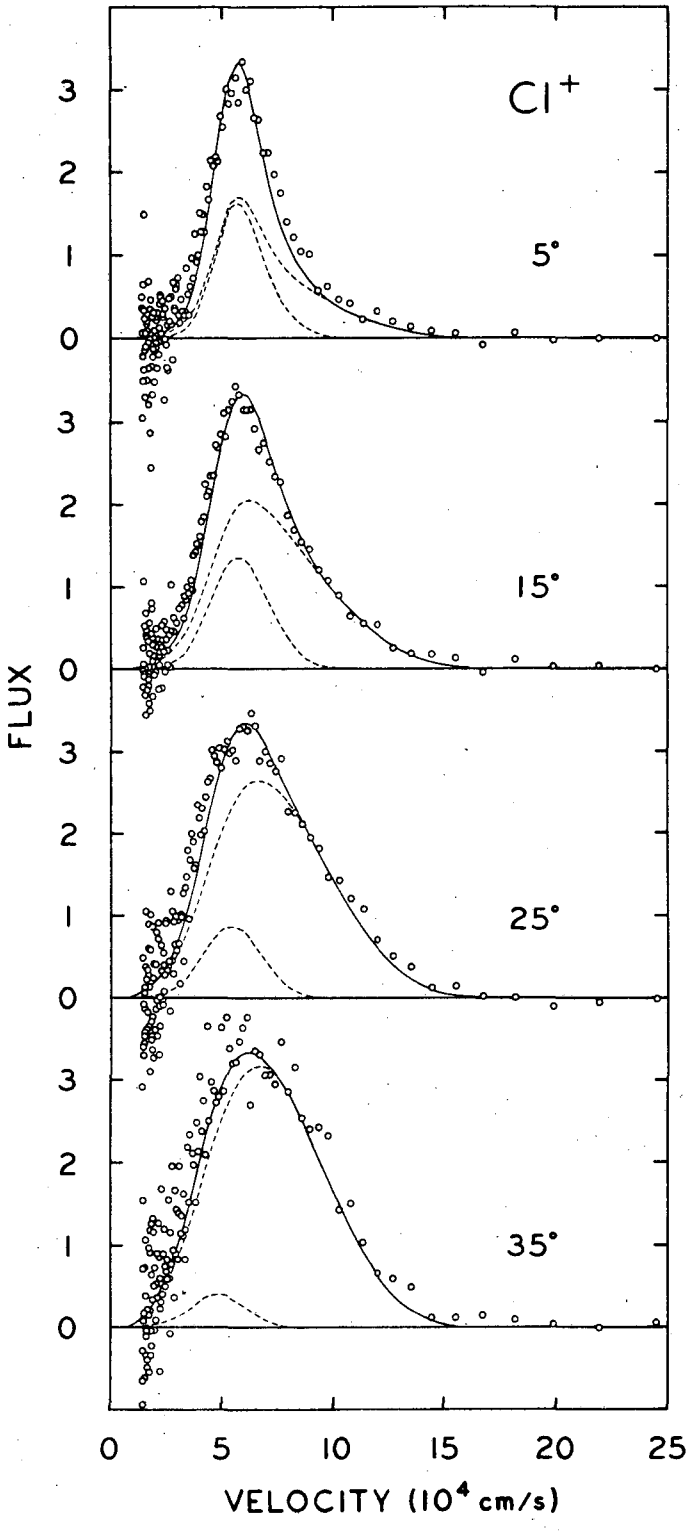
Cl+
5°
15°
25°
35°
FLUX
0
1
2
3
0
5
10
15
20
25
VELOCITY (10⁴ cm/s)
XBL 814-9369

Fig. 6

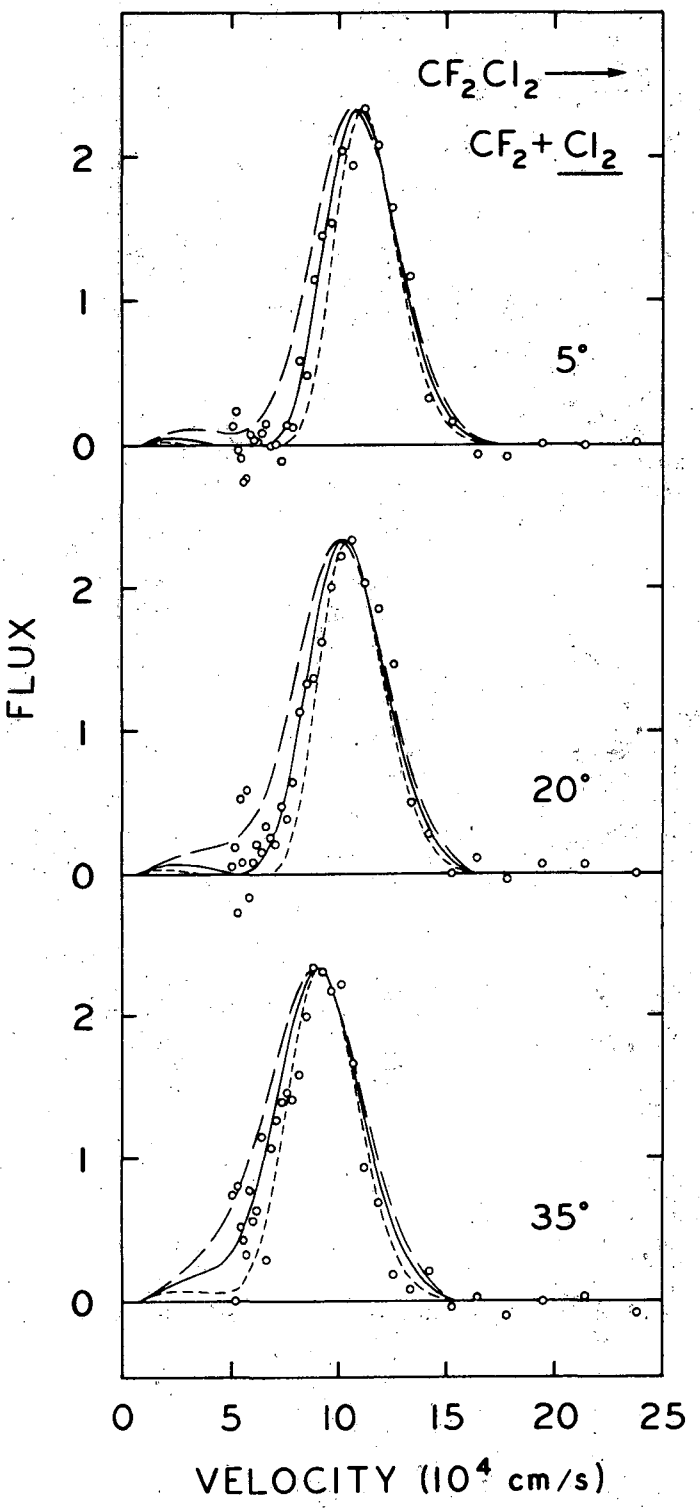
$CF_2Cl_2 \longrightarrow$
$CF_2 + Cl_2$
5°
20°
35°
FLUX
0
1
2
0
5
10
15
20
25
VELOCITY (10^4 cm/s)
XBL 814-9370

Fig. 7

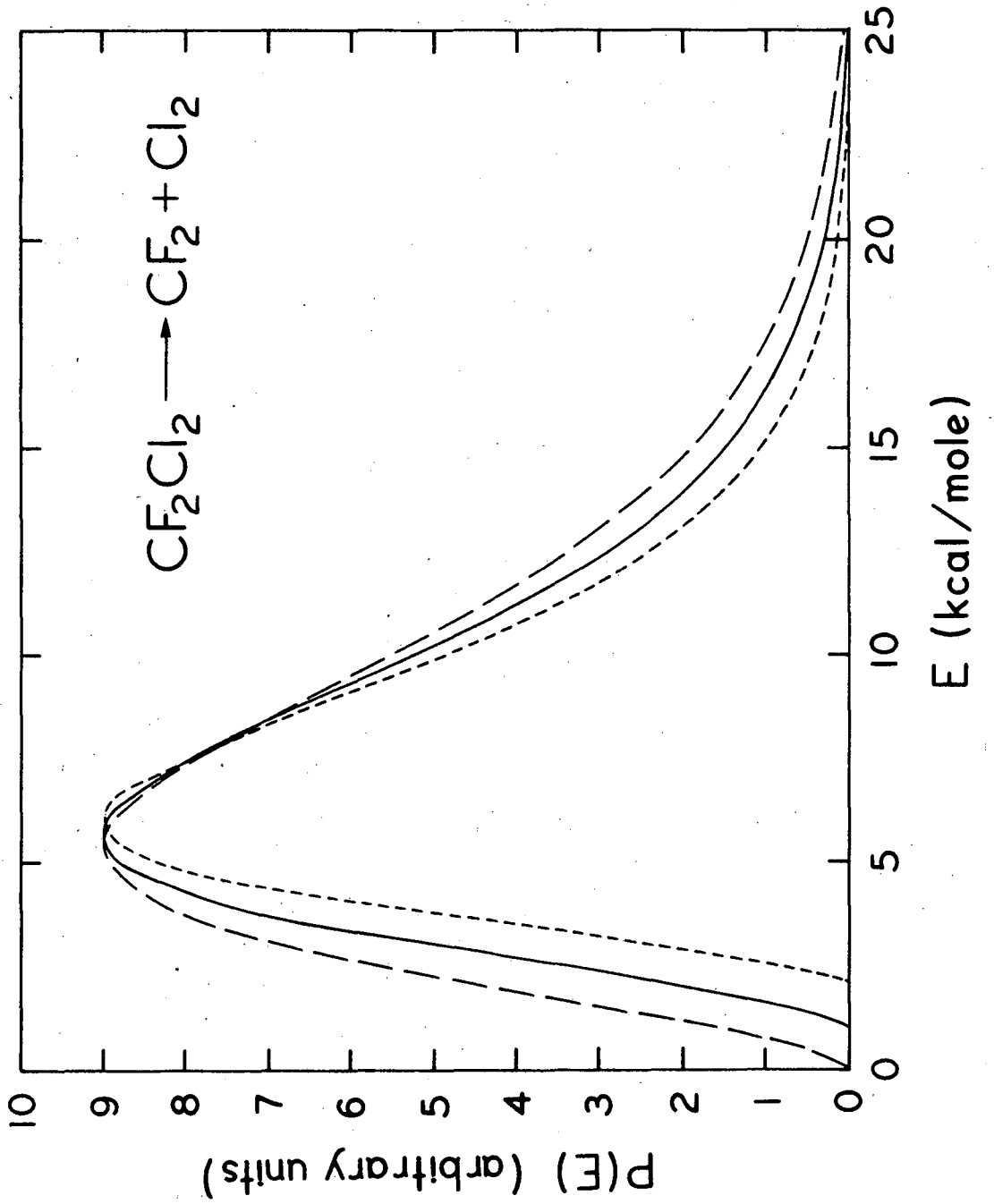

XBL 814-9366

Fig. 8

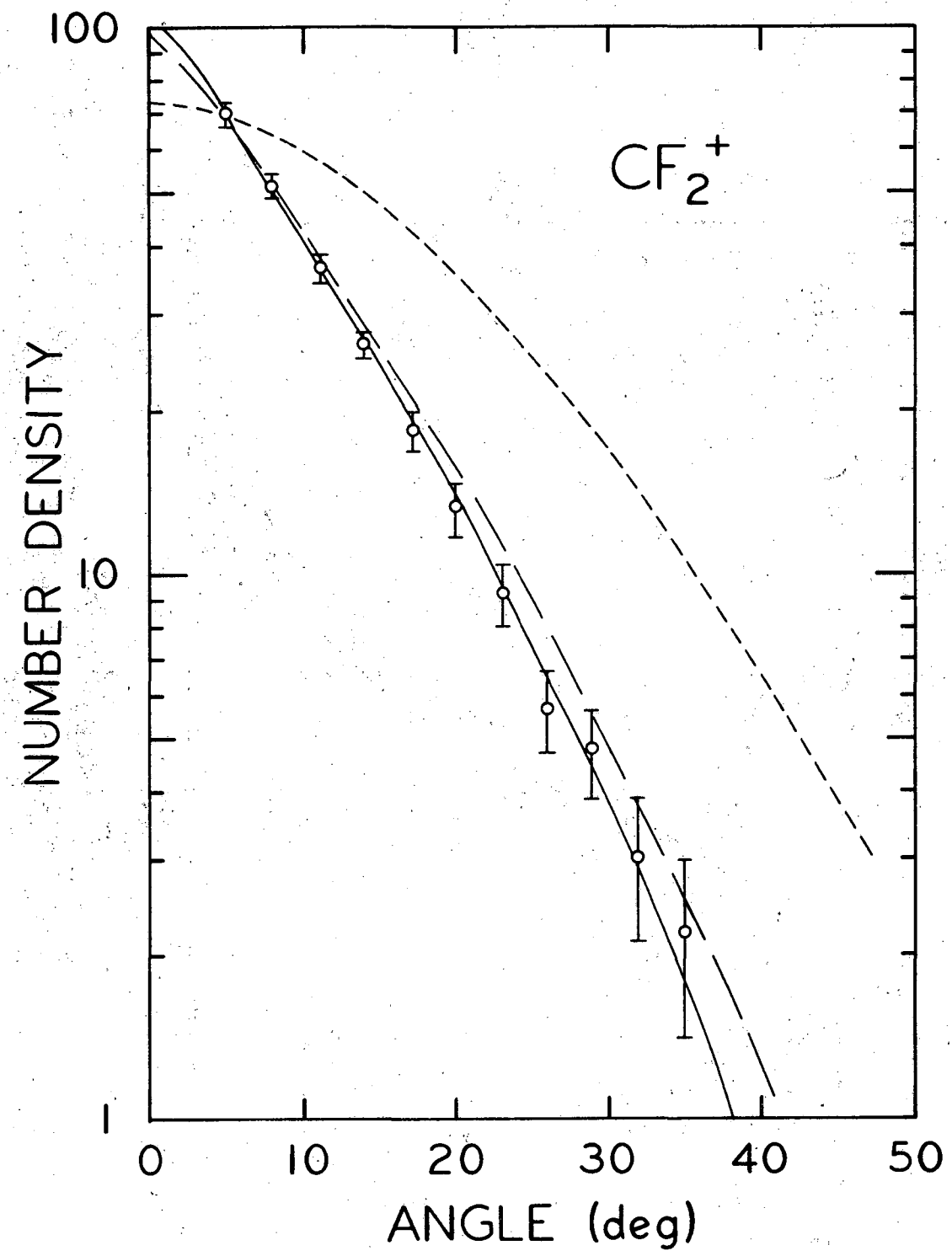

Fig. 9

XBL 814-9362

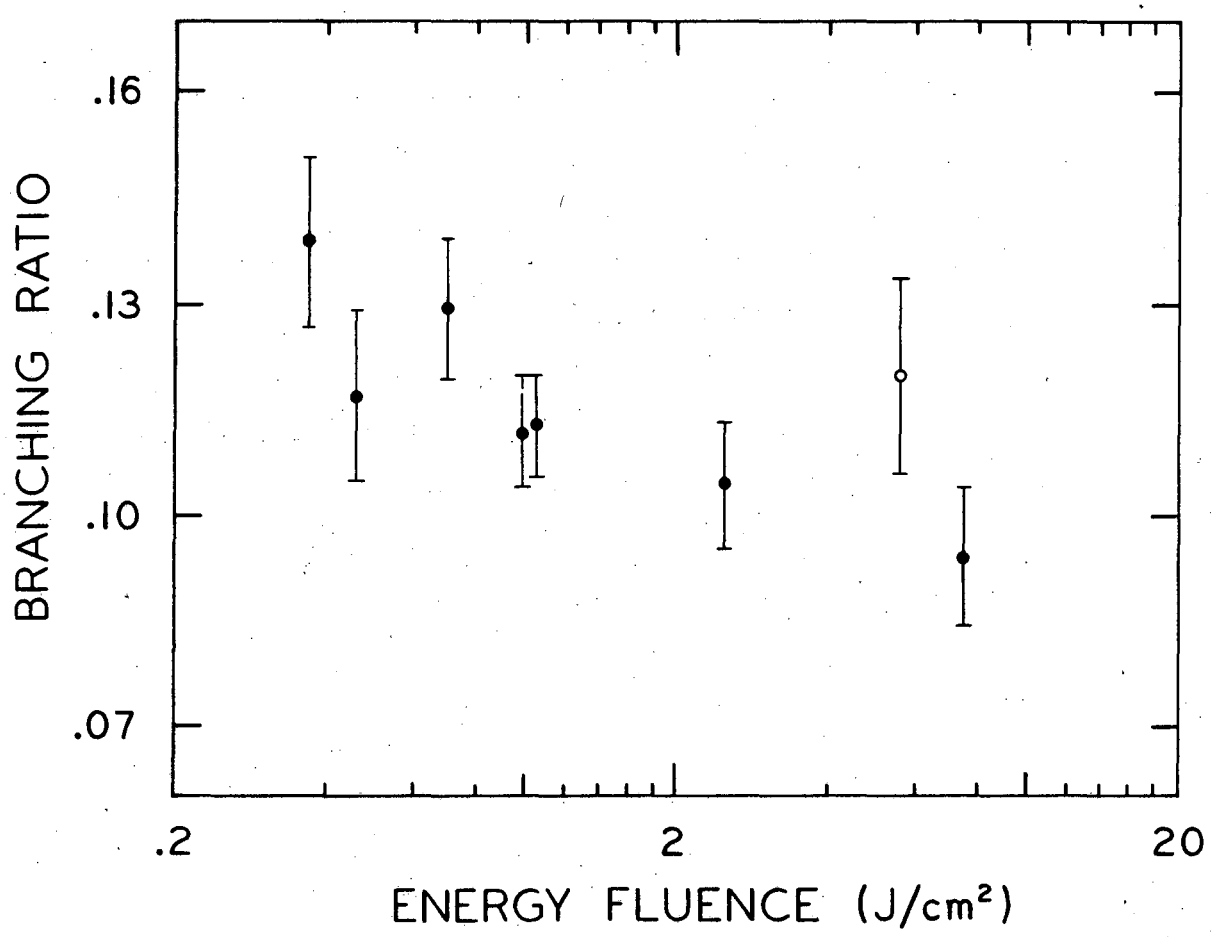

XBL 814-9361

Fig. 10

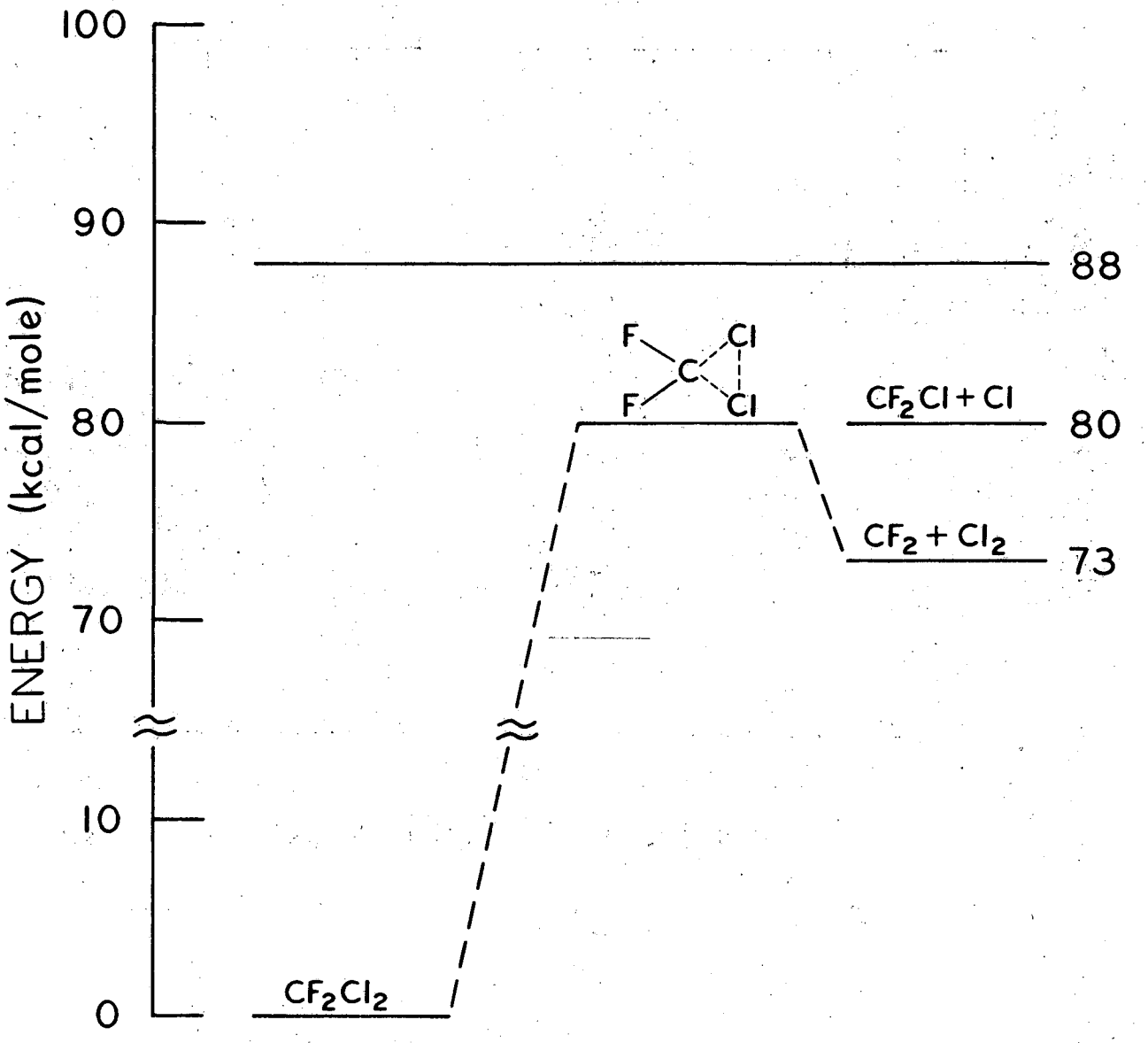

XBL 814-9364

Fig. 11

Appendix I: RRKM Calculations

The RRKM rate constant is given by

$$k(E^*) = \frac{g\, G(E^\dagger = E^* - E_0)}{h\, N(E^*)}$$

where E^* is the excitation energy, E_0 is the threshold energy for dissociation, $N(E^*)$ is the density of states for the molecule at energy E^*, $G(E^\dagger)$ is the sum of states available to the critical configuration at excess energy $E^\dagger$, g is the reaction path degeneracy (g = 2 for Cl elimination, g = 1 for Cl_2 elimination), and h is Planck's constant. $k(E^*)$ was evaluated using the computer code of Hase and Bunker. The energy thresholds for both the Cl and Cl_2 elimination reactions were set equal to 80 kcal/mole. Sums and densities of states were calculated in the harmonic approximation using the semiclassical Whitten-Rabinovitch approximation.[22] The frequencies used are listed in Table A1. For the Cl elimination reaction, one of the C-Cl stretching frequencies is lost in the critical configuration, and two bending frequencies were substantially lowered. For the Cl_2 elimination reaction, both C-Cl stretching frequencies are lost in the critical configuration and a Cl-Cl stretching frequency appears (which we set equal to the vibrational frequency of diatomic chlorine). The bending frequencies in the critical configuration were not changed from the corresponding molecular frequencies.

We also took into account the slight shift in the excess energy scale due to the difference in rotational energy between the molecule and critical configuration (treating the external rotations as adiabatic). Assuming r_{C-Cl} = 1.74 Å, r_{C-F} = 1.33 Å, and tetrahedral bond angles,

the principal moments of inertia of the molecule were calculated to be (in amu -Å^2): $I_{xx} = 124$, $I_{yy} = 220$, $I_{zz} = 186$. For the critical configuration of the Cl elimination reaction, we assumed one C-Cl bond was stretched to 3.0 Å, yielding $I^{\dagger}_{xx} = 138$, $I^{\dagger}_{yy} = 459$, $I^{\dagger}_{zz} = 411$. For the critical configuration of the Cl_2 elimination reaction, we kept both C-Cl bond lengths at 1.74 Å but reduced the Cl-C-Cl bond angle until the Cl-Cl distance equaled 2.0 Å (the equilibrium bond distance in Cl_2), yielding $I^{\dagger}_{xx} = 117$, $I^{\dagger}_{yy} = 194$, $I^{\dagger}_{zz} = 167$. At an assumed rotational temperature of 100°K in the molecular beam, the calculated differences in rotational energy between the molecule and crictical configuration were +0.24 and -0.03 kcal/mole for the Cl and Cl_2 eliminations, respectively. Thus, the effect of the adiabatic rotations is to increase slightly the rate of Cl elimination relative to Cl_2 elimination at a given (vibrational) excitation energy E*.

The above models lead to calculated high-pressure Arrhenius A-factors of $\log_{10}A = 15.4$, 13.4 for the Cl, Cl_2 elimination reactions at T = 1000°K. (In retrospect, the inclusion of the detail of the effect of adiabatic rotations does not really seem warranted, since we're guessing at the A-factors anyway.)

The results of the RRKM calculation are shown in Fig. A1. We would like to make several comments concerning the rate constant curves:

1. If the energy threshold, E_o, is changed slightly, then to a good approximation the k(E*) vs. E* curve retains the same shape, and is merely displaced horizontally.

2. If the critical configuration frequencies are altered, the rate constant curve again retains about the same shape, and is only displaced vertically.
3. Because of (1) and (2), changes in the branching ratio with excitation energy are mainly due to differences in the energy thresholds of the competing dissociation channels, not differences in the shapes of the rate constant curves. Actually, the basic shape of the rate constant curve is largely determined by the number of vibrational degrees of freedom in the parent molecule.
4. If anharmonicity is taken into account during the state counting, the effect is to decrease the RRKM rate constants (lengthen the lifetimes), since anharmonicity will increase the density of states of the molecule at energy E* much more than it will increase the sum of states available to the critical configuration at energy E* - E_0. However, since the branching ratio between two competing channels does not depend on the absolute value of N(E*), this quantity will not be greatly affected by anharmonic corrections.

Table A1. Frequencies used in RRKM calculations.

Molecular Frequencies (cm^{-1}) (Ref. 7)	Critical Configuration Frequencies (cm^{-1})	
	Cl elimination channel	Cl_2 elimination channel
1167	1167	1167
1098	1098	1098
923	--	--
667	667	560
458	458	458
446	446	446
435	435	435
322	68	322
262	55	262

Fig. A1. RRKM rate constant curves for Cl and Cl_2 elimination from CF_2Cl_2, assuming a threshold energy of 80 kcal/mole for both channels.

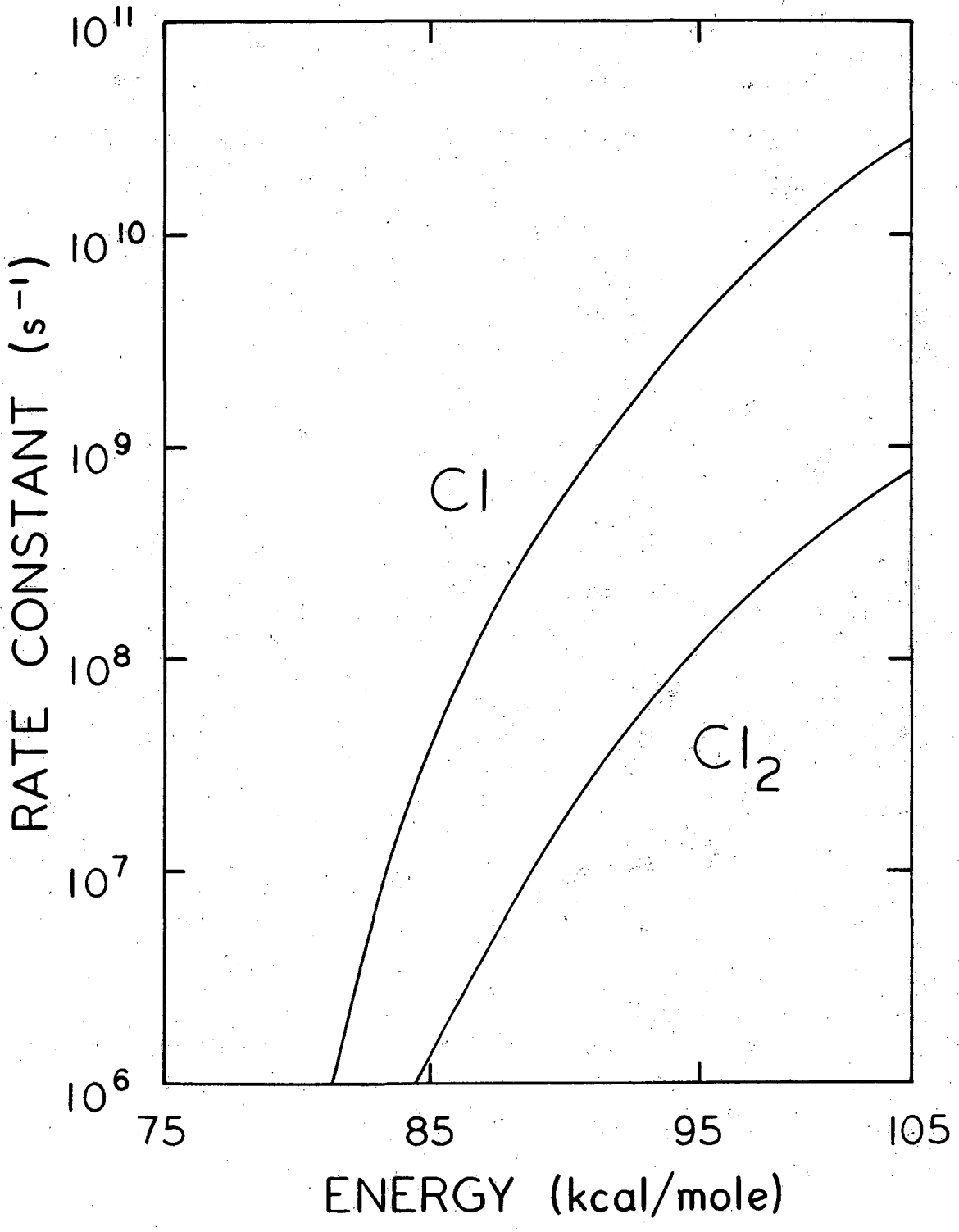

XBL 814-9363

Fig. A1

Appendix II: Relationship Between LAB and CM Product Ratios.

Consider two competing unimolecular dissociation channels of a parent molecule M:

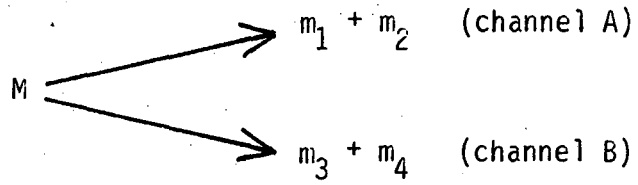

where $M = m_1 + m_2 = m_3 + m_4$.

Suppose that, in the laboratory, a beam of parent molecules is moving with velocity $\vec{v}_M$. At t = 0, some of the M molecules are energized by a laser pulse to a level which is above the threshold energies of both channels A and B. A number c_A of the energized molecules decompose through channel A, while the remaining c_B molecules decompose through channel B. The product branching ratio is given by

$$R = \frac{c_A}{c_B} .$$

In the CM reference frame (that is, to an observer traveling with velocity $\vec{v}_M$), the fragments from each dissociation channel will appear to recoil with characteristic translational energy and angular distributions. It is well established that in infrared multiphoton dissociation the CM product angular distribution is essentially isotropic. We will adopt this simplification here. Thus the ratio of the fluxes of any two products will be independent of angle in the CM coordinate system. This will not be true in the LAB.

Suppose we monitor fragment m_1 from channel A and fragment m_3 from channel B at a fixed laboratory angle θ (measured relative to $\vec{v}_M$).

Our goal is to calculate R from the measured m_1:m_3 signal ratio, assuming that we know the CM translational energy distributions for both dissociation channels.

For now just consider channel A. The quantity of greatest physical significance is the CM differential flux distribution in energy space, which is given by

$$\frac{dI_A^{CM}(E)}{dE} = c_A \cdot P_A(E),$$

where E is the combined CM translational energy of m_1 and m_2 and $P_A(E)$ is the normalized CM product translational energy distribution for channel A. ($P_A(E)$ has units of $(\text{energy})^{-1}$. $dI_A^{CM}(E)/dE$ has units of number of dissociation events (through channel A) per laser pulse per unit energy.)

The CM differential flux distribution of fragment m_1 in velocity space is

$$\frac{dI_A^{CM}(u_1)}{du_1} = c_A \cdot P_A(u_1),$$

where u_1 is the CM velocity of m_1 and $P_A(u_1)$ is the normalized CM velocity distribution for m_1. ($P_A(u_1)$ has units of $(\text{velocity})^{-1}$.) E is related to u_1 according to

$$E = \left[(1.19503 \times 10^{-3}) \frac{m_1 M}{m_2}\right] u_1^2,$$

where E is in kcal/mole, the masses are in amu's, and u_1 is in units of 10^4 cm/sec. We will drop the numerical factor, since we could always choose velocity units which would make this factor one.

Since flux is conserved,

$$\frac{dI_A^{CM}(E)}{dE}\,dE = \frac{dI_A^{CM}(u_1)}{du_1}\,du_1 ,$$

or equivalently,

$$P_A(E)dE = P_A(u_1)du_1.$$

Hence

$$P_A(u_1) = P_A(E)\frac{dE}{du_1} = \frac{m_1 M}{m_2}\cdot u_1 \cdot P_A(E).$$

The m_1 signal measured in the labortory at angle θ is given by

$$N_{m_1}^{LAB}(\theta) = \Gamma \int_{v_1=0}^{\infty} \frac{dN_{m_1}^{LAB}(v_1)}{dv_1}\,dv_1$$

where $dN_{m_1}^{LAB}(v_1)/dv_1$ is the LAB differential number density distribution of fragment m_1 in velocity space (at angle θ), v_1 is the LAB velocity of m_1, and Γ is an apparatus constant. (Recall that the ionizer is a number density detector.) The units of $N_{m_1}^{LAB}(\theta)$ are simply number of m_1 counts per laser pulse. Transforming from LAB number density to flux gives

$$N_{m_1}^{LAB}(\theta) = \Gamma \int_0^{\infty} \frac{dI_{m_1}^{LAB}(v_1)}{dv_1} \frac{1}{v_1} dv_1 .$$

The LAB and CM differential velocity flux distributions are related by the usual transformation Jacobian:[24]

$$\frac{dI_{m_1}^{LAB}(v_1)}{dv_1} = \frac{v_1^2}{u_1^2} \frac{dI_A^{CM}(u_1)}{du_1} .$$

Substituting in we get

$$N_{m_1}^{LAB}(\theta) = \Gamma \int_0^{\infty} \frac{dI_A^{CM}(u_1)}{du_1} \cdot \frac{v_1^2}{u_1^2} \cdot \frac{1}{v_1} dv_1$$

$$= \Gamma c_A \int_0^{\infty} P_A(u_1) \frac{v_1}{u_1^2} dv_1$$

$$= \Gamma c_A \frac{m_1 M}{m_2} \int_0^{\infty} P_A(E) \frac{v_1}{u_1} dv_1 .$$

If we go through the same procedure for fragment m_3 from dissociation channel B, we find that the m_1:m_3 signal ratio at angle θ is given by

$$\frac{N_{m_1}^{LAB}(\theta)}{N_{m_3}^{LAB}(\theta)} = \left(\frac{c_A}{c_B}\right)\left(\frac{m_1/m_2}{m_3/m_4}\right)\frac{\int_0^\infty P_A(E)\,\frac{v_1}{u_1}\,dv_1}{\int_0^\infty P_B(E)\,\frac{v_3}{u_3}\,dv_3}$$

$$= R\left(\frac{m_1 m_4}{m_2 m_3}\right)\frac{\int_0^\infty P_A(E)\,\frac{v_1}{u_1}\,dv_1}{\int_0^\infty P_B(E)\,\frac{v_3}{u_3}\,dv_3}\,.$$

This is the desired relationship between the product ratio measured in the LAB and the corresponding CM quantity.

TECHNICAL INFORMATION DEPARTMENT
LAWRENCE BERKELEY LABORATORY
UNIVERSITY OF CALIFORNIA
BERKELEY, CALIFORNIA 94720